

Paolo Blondeaux, Marco Colombini, Giovanni Seminara, Giovanna Vittori

Introduction to Morphodynamics of Sedimentary Patterns



Genova University Press
*Monograph Series **Morphodynamics of Sedimentary Patterns***

Editorial Board:

Paolo Blondeaux, Marco Colombini
Giovanni Seminara, Giovanna Vittori

Advisory Board:

Sivaramakrishnan Balachandar (*University of Florida U.S.A.*)
Maurizio Brocchini (*Università Politecnica delle Marche, Italy*)
François Charru (*Université Paul Sabatier, France*)
Giovanni Coco (*University of Auckland, New Zealand*)
Enrico Foti (*Università di Catania, Italy*)
Marcelo H. Garcia (*University of Illinois, U.S.A.*)
Suzanne J.M.H. Hulscher (*University of Twente, NL*)
Stefano Lanzoni (*Università di Padova, Italy*)
Miguel A. Losada (*University of Granada, Spain*)
Chris Paola (*University of Minnesota, U.S.A.*)
Gary Parker (*University of Illinois U.S.A.*)
Luca Ridolfi (*Politecnico di Torino, Italy*)
Andrea Rinaldo (*École Polytechnique Fédérale de Lausanne, Switzerland*)
Yasuyuki Shimizu (*Hokkaido University, Japan*)
Marco Tubino (*Università di Trento, Italy*)
Markus Uhlmann (*Karlsruhe Institute of Technology, Germany*)



Paolo Blondeaux, Marco Colombini, Giovanni Seminara, Giovanna Vittori

Introduction to Morphodynamics of Sedimentary Patterns





is the bookmark of the University of Genoa



UNIVERSITÀ DEGLI STUDI
DI GENOVA

On the cover:

The delta of Lena river (Russia). The image was taken on July 27, 2000 by the Landsat 7 satellite operated by the U.S. Geological Survey and NASA (false-color composite image made using shortwave infrared, infrared, and red wavelengths). Image credit: NASA



This book has been object of a double peer-review according with UPI rules.

Publisher

GENOVA UNIVERSITY PRESS

Piazza della Nunziata, 6 16124 Genova

Tel. 010 20951558

Fax 010 20951552

e-mail: ce-press@liste.unige.it

e-mail: labgup@arch.unige.it

<http://gup.unige.it/>

The authors are at disposal for any eventual rights about published images.

Copyrights are protected by law.

All rights reserved by copyright law



(eBook version)

ISBN: 978-88-97752-99-8 (eBook version)

Print on January 2018



Print

Centro Stampa - Università degli Studi di Genova - Via Balbi 5, 16126 Genova

e-mail: centrostamp@unige.it

Contents

1 The sediment journey from hillslopes to abyssal plains	11
1.1 Sediments	11
1.1.1 Sediment grains and sediment mixtures	12
1.1.2 Sediment yield	18
1.2 Sediment mobilization	19
2 Wandering through our sedimentary world: sedimentary patterns	29
2.1 Various paradigms to organize field observation	29
2.2 Hillslope patterns	32
2.3 Fluvial patterns	32
2.3.1 Free fluvial patterns: free bedforms	33
2.3.2 Forced fluvial patterns	38
2.3.3 Fluvial planforms	40
2.3.4 Fluvial patterns and river engineering	42
2.4 Transitional patterns	47
2.4.1 Transitional plan forms	47
2.4.2 Transitional bedforms	52
2.4.3 The impact of development on transitional environments.	53
2.5 Coastal patterns	56
2.5.1 Coastal bed-forms	57
2.5.2 Coastal planforms	63
2.5.3 Grain-sorting in coastal patterns	66
2.5.4 The impact of sedimentary patterns on coastal management	68
2.6 Deep sea patterns	70
2.6.1 Deep sea patterns and offshore engineering	74
3 Morphodynamics: a free boundary problem	79
3.1 The bed interface as a free boundary	79
3.2 Evolution equation of an erodible interface (Exner equation)	80
3.3 Exner formulation of the evolution equation	81
3.3.1 The local form of the mass conservation equation for the solid phase	81
3.3.2 Derivation of the 2-D Exner equation for homogeneous sediments	83
3.3.3 Extension to the case of heterogeneous sediments	87
3.4 Coupling the evolution of the erodible interface to the flow field	88

Introduction to the monograph series

The innovations brought up by technology in the last century and further progressing at the beginning of the third Millennium have profoundly affected the modes of scientific communication. Nowadays, the interaction among scientists occurs through a variety of web tools, whereby various schools of thought may influence each other at a rate much faster than in the past.

On the other hand, scientific books have become less fashionable for a number of reasons, two of them of major impact. Firstly, books are intrinsically conceived to present a 'static' knowledge, hence they are more appropriate to provide assessments of settled disciplines than to respond quickly to the 'dynamic' evolution of new or unsettled subjects. Secondly, their cost is often prohibitive both for research students, who are supposed to be their main users, and even for libraries.

However, there is an objective need for state of the art assessments of the knowledge built up in fields where research is intense and progress is significant. The more so when the subject is strongly interdisciplinary, i.e. it involves scientific communities that benefit from mutual interactions.

Morphodynamics is such a field. Originally developed at the boundary between geomorphology (Leopold and Wolman, 1957, Allen, 1982) and hydraulic engineering (Vanoni, 1975, Graf, 1984), it underwent a rapid development around the middle of the last century when various outstanding scientists of different schools refreshed the subject with the help of novel ideas. Then, Morphodynamics definitively moved from its previous descriptive-empirical status to become a branch of Fluid Mechanics in any respect. A few great names deserve to be mentioned, having marked this transition with their seminal contributions: R.A. Bagnold in Great Britain (Bagnold, 1966), J.F. Kennedy (Kennedy, 1969) and J. D. Smith (Smith, 1970) in the United States, F. Engelund (Engelund and Fredsoe, 1982) in Denmark, van Bendegom in The Netherlands (Jansen et al., 1994), K. Ashida (Ashida and Michiue, 1973) in Japan. Their work will be discussed and frequently quoted in the various monographs of this series.

Following the lead of these scientists, a number of groups of morphodynamics developed in engineering schools throughout the world. A new generation of leaders and their schools soon emerged, most notably in USA, Denmark, Japan

and The Netherland. The impulse of these scientists, their coworkers and a number of further groups, has led to a rapid growth of the morphodynamic community. A sequence of biennial meetings of River, Coastal and Estuarine Morphodynamics (RCEM), was then established in order to promote exchange of knowledge among the various schools. The first meeting was held in Genoa in 1999 and the tenth meeting of the series is scheduled to be convened in Padua this year. The distinct feature of these meetings is to provide a forum where cross-fertilization among geomorphologists, engineers, physicists and applied mathematicians could be pursued.

It is also fair to note that this interaction is not at all easy, for a variety of reasons. First of all, the viewpoint of geomorphology is often holistic: it is the functioning of the system as a whole that is the major concern of geomorphologists. And field observations are their primary tool. The engineering approach tends to be reductionist: understanding the system is a goal pursued through the analysis of its various components, with the help of physical and mathematical models. Hence, a problem of language arises unavoidably as the language of mathematics is not necessarily equally accessible to different audiences and may discourage their dialogue. Moreover, modeling is, by definition, a process whereby the complexity of systems is reduced, such to make the problem amenable to theoretical treatments. To what extent may simplification be accepted is not an obvious matter and different communities may have different feelings and tastes. This notwithstanding the dialogue must be pursued and tools must be constructed to make it increasingly feasible. The present series of monographs is an attempt in this direction.

With the above premise, let us clarify our goals.

Our aim is to construct an educational tool targeted mainly to PhD students involved in research on Morphodynamics. The flavor of our approach will be mainly theoretical but our ambition is to make it accessible to different scientific communities, although the effort needed will likely differ significantly depending on the community involved.

We feel that the tool '*series of e-monographs*' is to be preferred to the tool '*single comprehensive book*'. For a variety of reasons. Firstly, a series of e-monographs allows to analyze in depth a wide range of subjects in the general field of Morphodynamics. Secondly, e-monographs may be easily updated, i.e. they allow for a *dynamic* assessment of the available knowledge. Thirdly, they may be associated with a sort of 'scientific blog' allowing for an interaction between Authors and readers, a feature that may also lead to a dialogue between different schools of thought in a productive and instructive fashion. Finally, e-monographs may be made available free or at a very low price even if they contain a large number of color photos or pictures, that are essential in the present context. We have decided that the monographs of this series will be freely downloadable.

Note that each of the forthcoming monographs will be conceived as an independent body of knowledge: the reader will not need to acquire the knowledge contained in monograph A in order to be able to follow the content of monograph B, with only one possible exception: some basic knowledge on the mechanics of sediment transport is a preliminary tool needed to all readers who have no previous knowledge of the subject. Hence, our first planned monograph following the present introductory monograph is an up to date assessment of the state of the art on the mechanics of sediment transport in subaqueous environments.

Our approach implies that there may be some overlap among topics treated in different monographs. An example: fluvial free bars are one of the instabilities of free surface flow over a mobile bed, hence they will be thoroughly discussed in a monograph specifically dedicated to fluvial bedforms. However, free bars also play a major role in river meandering. Hence, some (less detailed) knowledge on free bars must also be contained in the monograph dedicated to river meandering. Treatments may also differ slightly in different monographs. We do not see this as a problem: on the contrary, readers may find it instructive to see the same problem taken from possibly different viewpoints. Also, we do not need to employ exactly the same notations in different monographs, although an effort will be made to make the language as uniform as possible, such that the collection of all monographs will hopefully provide a coherent picture.

Genova, September 2017
The Editorial Board

Chapter 1

The sediment journey from hillslopes to abyssal plains

In order to set the scene for the analysis pursued in the present series of monographs, it is preliminarily useful to become familiar with the main actor of our play, namely sediments. We first provide some elementary knowledge on their characteristics and then describe the motion of sediments from the sites where they originate down to their final destination, i.e. the abyssal plains.

1.1 Sediments

Sediments are naturally produced in the upper parts of river basins through a number of physical mechanisms: notably, *weathering of rocks* due to chemical, mechanical or organic factors and detachment of material from the surface of soil mantled landscapes. Detachment occurs dominantly as mass movements, either in the form of *creep* (a slow process caused by bioturbation, frost heaving and wetting-drying cycles) or in the form of *landsliding*. Further sediments are naturally produced by *hillslope erosion* driven by overland flow.

Sediments are also artificially produced by anthropogenic sources, that may have a major impact on the sediment budget of watersheds. Among the major anthropogenic contributions, *soil loss from croplands*, *deforestation* and *mining activities* play an important role. An example may help the reader appreciate the importance of anthropogenic sources. The well known Carrara marble is mined from the Apuane Alps, a chain of mountains adjacent to the Tuscanian coast in the north of Italy. The major river draining the Apuane Alps is called Carrione: its watershed has an area of about 47 Km². In 2008, as many as 167 mines were located in the Carrione watershed, 90 of them being active (Cortopassi et al., 2008). They produce an amount of detritus as large as 3 Mtons/year (Baroni et al., 2010). This material is partly dumped on the hillslopes surrounding the mines

and partly stocked (figure 1.1). Part of the fine material is removed by overland flow associated with storm events, contributing to increase the sediment supply to the river which, due to this overload and the presence of levees in its valley reach, has become pensile whilst the adjacent floodplain is subsiding.



Figure 1.1: Image of marble mines of the Apuane Alps, where 3 Mtons of detritus is produced each year.

In nature, 90% of the rocks consist of *silicates*, mostly *feldspars and quartz*, namely the most diffused minerals of igneous rocks, both intrusive (*granites*) and diffusive (*basalts*). Silicates are also present in some sedimentary rocks like *sandstones*. Other minerals are less abundant in the earth crust. In particular *carbonates*, like *calcite and dolomite*, are basic constituents of sedimentary rocks like *limestones and dolomites*. Limestones are weakly resistant rocks that degrade easily into silt: hence, these sediments are hardly found far from their source.

1.1.1 Sediment grains and sediment mixtures

The specific weight of grain particles depends on their mineral composition, hence on the type of parent rock they derive from. Most minerals have *relative densities* in the range 2.6 – 2.9 (see Tab. 1.1). Few minerals, e.g. those containing *magnetite*, are much heavier.

Grains display a variety of shapes, derived from their formation process (magma crystallization, rock degradation, etc.) and the subsequent abrasion they undergo as they move downstream. *Shape factors* have been introduced to characterize

Material	Relative density
Aragonite	2.9
Granite	2.6-2.7
Siltstone	2.6-2.8
Basalt	2.7-2.9
Olivine	3.2
Coal	1.3-1.5

Table 1.1: Relative density of a few materials.

	Diameter d (mm)	$\phi = \lg_2 (d_r / d)$
Boulders	256-4096	-8, -12
Pebbles	64-256	-6, -8
Gravel	2-64	-1, -6
Sand	1/16-2	4, -1
Silt	1/256-1/16	8, 4
Clay	1/4096-1/256	12, 8

Table 1.2: Classification of sediment sizes according to Wentworth (1922).

the grain shape. In particular, the Corey factor is the ratio c/\sqrt{ab} , with a , b , c lengths of the major, intermediate and minor axes of an ellipsoid approximating the actual grain respectively (Corey, 1949). It takes typically values around 0.7. Alternatively, *sphericity* is defined as the ratio between the area of the surface of a sphere with volume equal to the volume of the grain and the area of the grain surface.

As particle shape is irregular, particle size is conventionally defined. *Sieving* is employed for particle size in the range 1/16-16 mm and in this range *particle diameter* is defined by the length of the square mesh of the sieve. For particle sizes smaller than 1/16 mm *settling* is employed: particle diameter is then defined as the diameter of a sphere with the same specific weight settling in water with the same speed under the same conditions. For particle sizes larger than 16 mm particle diameter is measured by *immersion* and is defined as the diameter of a sphere that, when immersed, displaces the same water volume. Finally, the size of large boulders can only be estimated, measuring the length of the intermediate axis of an ellipsoid taken to approximate the boulder. Further modern techniques (e.g. optical techniques appropriate to fine particles) are reviewed by Diplas et al. (2008).

Based on the above definitions, various classifications of sediment sizes have been proposed. In Tab. 1.2 the classic Wentworth classification (Wentworth, 1922) is reported.

Note that this Table reports both the grain diameter expressed in mm and the equivalent *sedimentological scale* ϕ , defined in the form:

$$d = d_r 2^{-\phi} \quad (1.1)$$

where d is the grain diameter and d_r is a reference diameter conventionally set equal to 1 mm. ϕ is a dimensionless variable defined in the interval $(-\infty, \infty)$. Positive (negative) values of ϕ correspond to diameters smaller (larger) than 1 mm, i.e. d increases as ϕ decreases.

The sedimentological scale maps the interval of observed diameters (which spreads over several decades) into a much more restricted ϕ interval. However, the definition (1.1) is somewhat awkward as grain size decreases if ϕ increases. It appears more convenient to introduce a ψ variable in the form

$$\psi = -\phi. \quad (1.2)$$

An important property of a sediment mixture is its *grain size distribution*. Let us define the *cumulative distribution function* for grain size $F(\psi)$ such that a fraction $F(\psi)$ of the sample weight contains sediment finer than d . By definition, it follows that

$$F(+\infty) = 1, \quad F(-\infty) = 0. \quad (1.3)$$

Similarly, one defines a distribution density function $f(\psi)$ in the form:

$$f(\psi) = \frac{dF}{d\psi}. \quad (1.4)$$

Note that $f(\psi)$ satisfies the integral constraint:

$$\int_{-\infty}^{\infty} f(\psi) d\psi = 1. \quad (1.5)$$

Then, based on the above definitions, one can readily define a few useful parameters suitable to characterize the mixture.

- ii) *Average diameter* d_{50} : diameter such that 50% of the sample weight is composed of grains finer than d_{50} .

In general, this definition can be extended to any diameter d_x (with x in the interval $0 - 100$). Hence:

$$F(d_x) = \frac{x}{100}. \quad (1.6)$$

ii) *Geometric mean d_g and standard deviation σ_g .*

The definition of these quantities is based on the first and second moment of the distribution density function $f(\psi)$:

$$\bar{\psi} = \int_{-\infty}^{\infty} \psi f(\psi) d\psi, \quad \sigma_{\psi}^2 = \int_{-\infty}^{\infty} (\psi - \bar{\psi})^2 f(\psi) d\psi, \quad (1.7a, b)$$

hence

$$d_g = d_r 2^{\bar{\psi}}, \quad \sigma_g = 2^{\sigma_{\psi}}. \quad (1.8a, b)$$

The value of σ_g is a measure of sediment gradation.

Below, we report some examples of grain size cumulative distribution functions typical of different sedimentary environments.

Gravel bed rivers contain both coarse and fine fractions, a feature that is often described saying that their grain size distribution is *bimodal*. Typical cumulative distribution functions (e.g. see figure 1.2) are upward concave (except for the upper diameter range). Moreover, the surface layer of gravel bed rivers (their *pavement*) is typically significantly coarser than their substrate. This is described as *bed armouring* and is clearly displayed in figure 1.2.

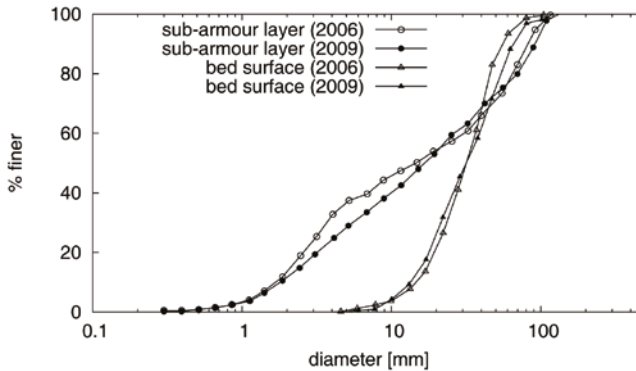


Figure 1.2: Cumulative grain size distribution typical of gravel bed rivers: sample collected close to the mouth of the Versilia River, Italy (adapted from Francalanci et al. (2013)).

Moving downstream, river beds undergo a process of bed fining. A cumulative distribution function typical of *sandy rivers* is reported in figure 1.3: it represents a nearly uni-sized (homogeneous) mixture with grain sizes falling in the range 0.3 – 0.5 mm and the practical absence of silt and gravel.

Finally, an interesting characteristic of the grain size distributions observed in fluvial environments is the absence of a significant content for fractions in the range 1 – 10 mm (the *granulometric gap*, figure 1.4). An important consequence is the occurrence of typically sharp transitions from river reaches with $d_{50} > 10$ mm to reaches with $d_{50} < 1$ mm, the so called *gravel-sand transition* which is also associated with sharp morphological changes.

Sediment mixtures are also characterized by a distinct porosity, λ_p , defined as the ratio between the volume of voids in a sample of the mixture (of linear

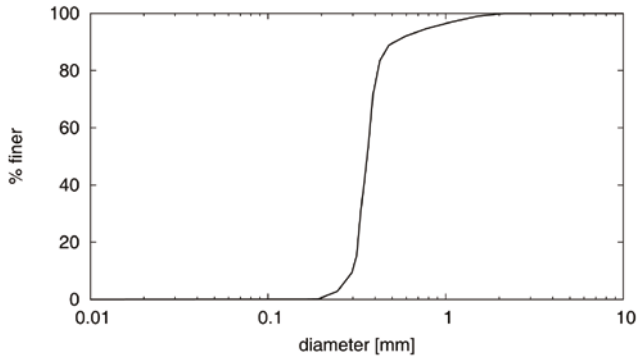


Figure 1.3: Cumulative grain size distribution typical of sandy rivers

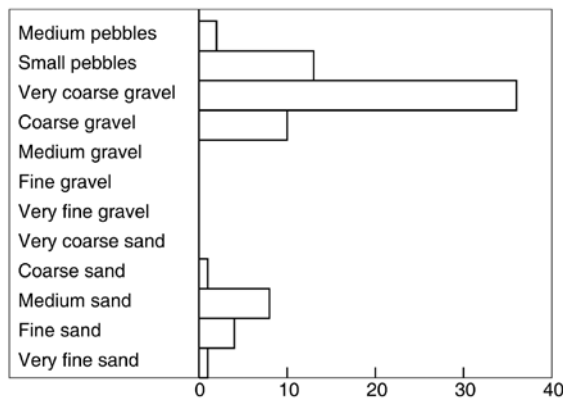


Figure 1.4: The histogram shows the frequency of different values of d_{50} of the surface layer observed in 78 rivers of the region of Alberta, Canada (modified from Parker and Peterson (1980)).

scale much larger than the grain size) and the volume of the sample. Sediment mixtures in natural environments have porosities depending on the grain shape as well as on their grain size distribution. For sandy mixtures values of λ_p are in the range 0.3 – 0.4. In gravel mixtures, voids are typically filled with finer material, hence porosity may decrease down to values around 0.2, depending on the percentage of fines.

Artificial granular media composed by grains of regular shape have porosities depending on grain arrangement, e.g.: spheres in the cannon ball (tetrahedron) arrangement (Fig. 1.5a) have minimum porosity, equal to 0.26, spheres in the cubic arrangement have much larger porosity, equal to 0.48 (Fig. 1.5b).

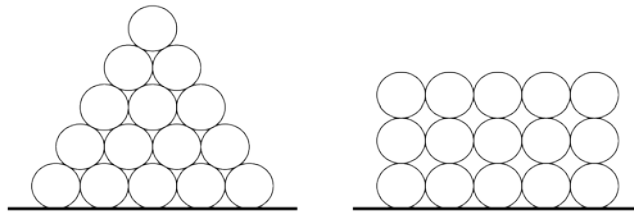


Figure 1.5: Artificial granular medium consisting of spheres in the cannon ball (tetrahedron) (a) or cubic (b) arrangement.

Porosity may vary significantly in time: this is the case of clay deposits that are initially characterized by fairly high porosity. Then, they undergo *consolidation*, a process whereby water contained in the interstices of the mixture is slowly expelled, leading to significant reduction of the mixture porosity. Temporal dependence of the mixture porosity may also arise from the effects of biological processes.

Note that the porous characteristic of gravel mixtures only affects the time scale of morphodynamic processes, that evolve otherwise independently of the absolute value of porosity. On the contrary, gravel porosity plays a crucial role in relation to the creation of suitable habitats for biological species like salmon.

1.1.2 Sediment yield

An estimate of global soil erosion based on the GLASOD (Global Assessment of Soil Degradation) survey (Oldeman et al., 1991, Walling and Webb, 1996) sets the sediment yield at 10^{11} t/yr, with a percentage of eroded soil delivered to the ocean (the so called *sediment delivery ratio*) of about 20%.



Figure 1.6: Satellite view of the gullied loess region drained by the Huangfuchuan River, a small tributary of the Yellow River dissecting the loess Plateau (Google Maps)

The reported values of the specific suspended sediment yield fall within a range spanning several orders of magnitude. Maximum annual values may be as high as few tens of thousands of t/Km^2 . Such peaks are reported for the Huangfuchuan River (Sui et al. (2008)), a relatively small tributary of the Yellow River in its middle reach, which drains a gullied region known as the loess plateau (figure 1.6). The high value of the specific sediment yield in this case is associated with a highly erodible terrain, lack of vegetation, intense storms coupled with a semiarid climate. In other contexts (e.g. Kenya) overgrazing also plays a major role, while steep mountainous relief, coupled with tectonic activity, high rainfalls and intense agricultural exploitation is characteristic of Taiwan, Java and New Guinea. The same mechanisms are present in New Zealand, where precipitations may reach annual values as large as 9000 mm. Minimum values of the specific annual sediment yield may be smaller than $1 t/Km^2$ (roughly 0.0004 mm) and are typically associated with highly resistant terrains, good vegetation cover and very low relief.

The figure 1.7 (Walling and Webb, 1983) shows that the sediment yield is highest in the loess region of China, along the mountain area of the Pacific margin, in regions with mediterranean and semi-arid climates and, finally, in the tropical areas.

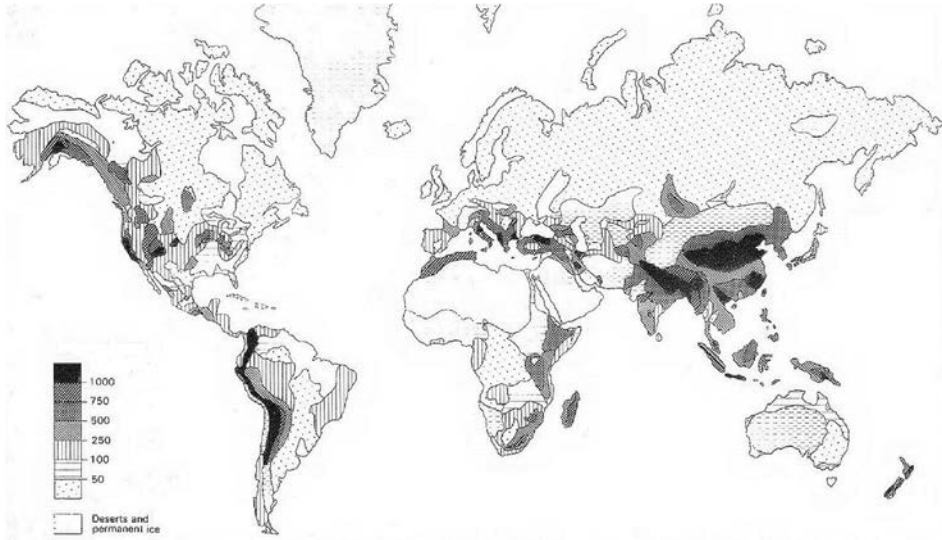


Figure 1.7: Suspended sediment yield ($\text{t km}^{-2} \text{ yr}^{-1}$) (adapted form Walling and Webb (1983)).

1.2 Sediment mobilization

Once the sediment is produced, it can be mobilized through a variety of mechanisms.

Gravity driven mass flows

On steep slopes sediment motion takes typically the form of gravity driven mass flows. Earthquakes or rapid snow melt may trigger surges of dry material known as *rock slides and rock avalanches*, which are also occasionally observed in the absence of a clear triggering event, being possibly associated with gradual stress release. The glacial Yosemite Valley, bounded by steep granite cliffs, provides a typical environment where several rock slides occur each year such that the rock debris accumulated at the base of some cliffs is over 100 m thick.

Heavy rains are capable to destabilize mixtures of coarse material embedded in a muddy matrix to give rise to the so called *mud flows and debris flows*. The figure 1.8 shows the result of a severe mud flow occurred in the Sarno area (south of Italy) on May 5 1998. It originated from a sequence of shallow landslides which mobilized the pyroclastic layer deposited on the underlying carbonatic rocks during the Vesuvio eruption of 79 B.C Mudflows are mainly composed of mud and silt.

They are typically triggered by extremely heavy rains or a sudden thaw, though in the Sarno event precipitations were persistent but not extreme (roughly a 10-15 years event).

When the source of sediments is deposition of pumice and ash erupted from volcanoes, then the resulting process is called a *lahar*. The figure 1.9 shows one of the most catastrophic lahars ever observed. It occurred at Mount St. Helens,



Figure 1.8: One of the mud flows occurred in the Sarno area (South of Italy) on May 5 1998 (Source: *Site polaris.irpi.cnr.it*, of Istituto di Ricerca per la Protezione Idrogeologica (IRPI), del Consiglio Nazionale delle Ricerche (CNR)).



Figure 1.9: The lahar occurred at Mount St Helens. Credit: U.S. Geological Survey Department of the Interior/USGS U.S. Geological Survey/photo taken on March 21, 1982 by Tom Casadevall.

as a result of an explosive eruption occurred on March 19, 1982. Pumice and ash reached an elevation of 14 kilometers resulting in a lahar flowing from the crater into the North Fork Toutle River valley eventually reaching the Cowlitz River, 80 kilometers downstream.

Mass flows may also be very slow motions of frozen debris as in the case of *rock glaciers* (figure 1.10). Rock glaciers are masses of rock cemented with interstitial ice, which behave like highly viscous fluids: essentially, water enters a pile of rocks and freezes underground, forming a permafrost interconnecting the rocks. As a result, ice builds up until it mobilizes the rock mass, which then flows downhill albeit quite slowly.

The common feature of the above phenomena is the dominant mechanism of sediment motion, originating from a balance between gravity and inter particle friction, with hydrodynamic forces playing a fairly minor role.

Hydrodynamically driven fluvial transport

A small part of the material eroded in the upper part of river basins, ranging roughly between 10% and 20%, reaches the river networks where bed slope typically experiences an abrupt reduction. At this stage, the dominant agent of sediment motion ceases to be gravity; rather, sediment particles exposed on the river bed may be destabilized by the action of hydrodynamic forces. In other words, sediment is transported by the flow as long as the latter is sufficiently intense to be able to mobilize bed particles.

Hydrodynamic transport is dominant throughout the rest of the fluvial journey of sediment particles. However, the river network does not simply

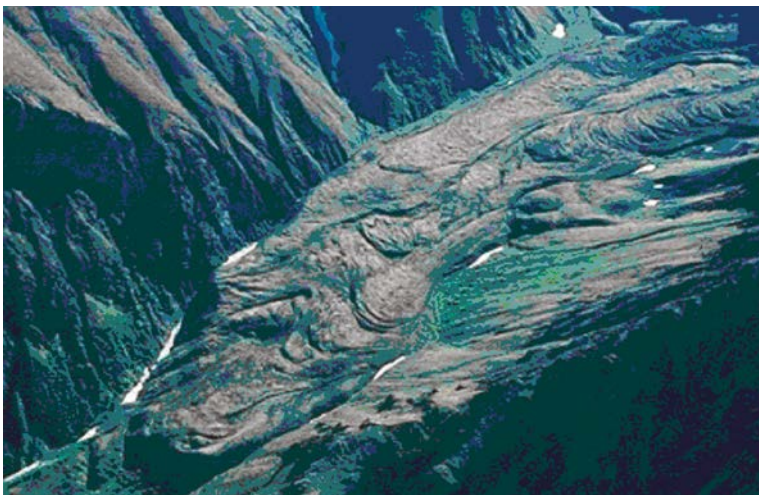


Figure 1.10: Rock glacier from the valley of Metal Creek in the Chugach Mountains of Alaska (Source: [wikimedia.org/wikipedia/commons/e/ed/Glacierrock1.gif](https://commons.wikimedia.org/wiki/File:Glacierrock1.gif)).

act as a conveyor belt for the sediments supplied by the upper river basin. The sediment load delivered by the fluvial stream is continuously modified as a result of a number of processes. Firstly, the river exchanges sediments with the flood plain: fine material, transported in suspension, settles in the flood plain when the stream flows overbank; material eroded from the banks or originated from bank collapse (figure 1.11a) is added to the sediment load at the expense of the floodplain; conversely, bank accretion is driven by sediment load carried by the stream and deposited at inner bends, where it may progressively consolidate as vegetation grows (figure 1.11b).

Secondly, proceeding downstream, the grain size distribution of the river bed undergoes progressive fining, as a result of the processes of selective sorting and particle abrasion. Gravel bed rivers (figure 1.12a) are typical of the upper part of the watersheds. As discussed in Section 1.1.1, they are characterized by poorly sorted sediments. Sandy streams dissecting the floodplains (figure 1.12b),

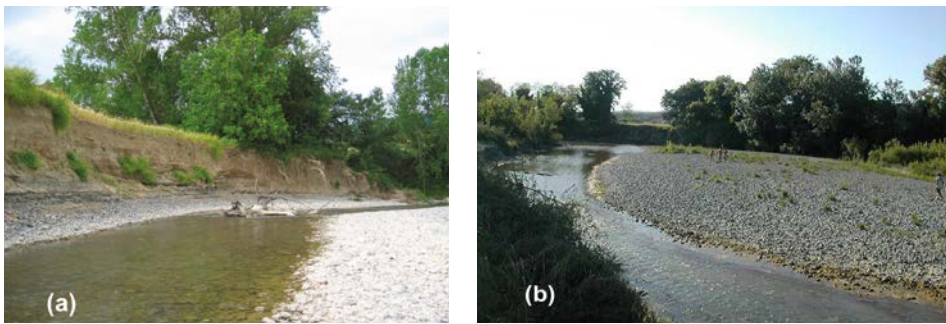


Figure 1.11: (a) Bank erosion at an outer bend of the Cecina River, Tuscany (Italy). (b) A typically unvegetated bar of the Cecina River, Tuscany (Italy), subject to prolonged exposure in drought conditions, may allow for the establishment of vegetation (courtesy of Luca Solari)



Figure 1.12: (a) Gravel bed of a reach the upper Magra river (Tuscany, Italy) Source: Seminara et al. (2012); (b) Sand bed reach of the Po River during the severe summer 2017 drought. Credit: Agenzia DIRE (<http://www.dire.it/23-06-2017/129616-siccita-italia-a-secco-tre-regioni-in-codice-rosso-fiume-po-sotto-la-media-di-15-metri/>)

have typically lost most of the coarse component of the bed material and are characterized by well sorted fine sediments.

Sediment motion in transitional environments.

Transitional environments, namely deltas and estuaries, are those regions where rivers meet the oceans. Further transitional environments are coastal lagoons, enclosed regions that exchange saline water with the ocean through inlets and (possibly) fresh water with the inland through rivers debouching into them.

In these regions, sediment is still transported hydrodynamically, but with a few novel ingredients. Firstly, the flow field and sediment transport may be significantly affected by tides, winds and waves. Secondly, the bed may be partially cohesive as it may contain a non negligible clay component. A third important feature is the possible presence of halophytic vegetation (figure 1.13) within morphological structures called *salt marshes*, which affect both the



Figure 1.13: (a) Image of a clump of *Spartina alterniflora*. (Source: USDA, NRCS. 2017. The PLANTS Database (<http://plants.usda.gov>, 11 July 2017). National Plant Data Team, Greensboro, NC 27401-4901 USA.); (b) Rushes and reeds in a salt marsh of Venice lagoon

hydrodynamics and the morphodynamics of transitional environments. Indeed, vegetation enhances hydrodynamic dissipation, hinders sediment resuspension by wind waves and tidal currents and drives sediment trapping. Moreover, the life cycle of biomass gives rise to the production of *organic sediments*, which then undergo compaction and contribute to the ability of wetlands to keep up with sea level rise.

The outcome of these novel features is a variety of landscapes characteristic of these environments, which will be presented in Section 2.4.

Sediment motion in coastal regions.

Sediment reaching the coastal area does not originate only from fluvial transport. It also derives from other sources. For example marine sediments may be produced by the erosion of coastal bluffs composed of glacial till (a mixture of clay, sand, gravel and cobbles left behind by glaciers). They may also derive from the decomposition of the shells and skeletons of marine organisms (see figures 1.14, 1.15 and 1.16), from the deposition of volcanic ash and lava originating from volcanoes located close to the coast (see figure 1.17), from sediment generated by cliff erosion (see figure 1.18), or from eolian offshore transport to the coastal region of sediments entrained from inland desertic regions.



Figure 1.14: Shell beach, Shark bay, Western Australia: one of the only two beaches entirely composed of shells, world heritage site. a) photo by Gabriele Delhey, taken from: https://commons.wikimedia.org/wiki/File:Shell_Beach.JPG; b) photo taken from: https://commons.wikimedia.org/wiki/File:Shell_Beach_Western_Australia.jpg#filelinks.

The sediment budget that controls the temporal evolution of coastlines thus involves a number of contributions. Usually, the one driven by longshore currents from adjacent areas is one of the largest. The contribution of rivers is also significant, although sediments are delivered intermittently, mostly during floods. The contribution of material eroded from bluffs and cliffs is also significant.

Various mechanisms contribute to the latter process: breaking waves smashing against the coast during storms; impact of flying sand grains and small pebbles against the cliff face; waves that, impacting against the coast, compress the air trapped in joints and cracks and weaken/erode the cliff face; weak acids contained in the sea water dissolving limestone and chalk possibly present in coastal rocks. A positive contribution to the coastal budget may arise from onshore transport and deposition driven by constructive waves. Finally, tidal currents as well as wind currents add their effects on sediment transport.



Figure 1.15: Pink beach at Budelli Island (Italy), photo by Esetto. The fragmented skeletons of the micro-organism that live on *Posidonia* cause the characteristic color of the sand (source: https://commons.wikimedia.org/wiki/File:Spiaggia_di_Budelli.jpg).



Figure 1.16: Sand beach, Irimote Island, Japan: its 'sand' is peculiar, being composed by small crustacean shells with star shape. (a) GFDL+creative commons2, (https://commons.wikimedia.org/wiki/File:Hoshizunano-hama_Irimote_Island04bs3s4592.jpg) b) labormikro/Creative Commons).



Figure 1.17: Papakolea beach, Hawaii: the beach has a green color, deriving from the presence of a greenish mineral (olivine) contained in the Hawaii lava. (a) photo by jonny-mt-Own work, CC BY 3.0, <https://commons.wikimedia.org/w/index.php?curid=4523258>; b) photo by Wilson44691-Own work, CC0, <https://commons.wikimedia.org/w/index.php?curid=40566540>).



Figure 1.18: Black beach of Punta Corvo (La Spezia, Italy). The color of the sand is due to the fragmentation of black cliffs surrounding the pocket beach (courtesy of Gian Luca Sgaggero; source: <https://www.viaggiaescopri.it/punta-corvo-spiaggia-emozioni-liguri/>).

It is observed that the processes of transport and erosion/deposition of sediments within the coastal margin are mainly contained within 'littoral cells'. It is also customary to assume that each cell is a closed system which does not exchange any sediment with adjacent cells. The boundaries of the littoral cells are determined by the shape of the coastline and the local topography. In particular,

large scale morphological features (e.g. peninsulas) are assumed to act as natural barriers that do not allow the transfer of sediment. Needless to say, this is just a useful idealized picture of reality, as some sediment is unavoidably exchanged between adjacent cells.

Sediment motion in submarine environments

In the last stretch of their journey towards the abyssal plains, sediments are transported by *turbidity currents* and the transport mechanism involves both gravitational and hydrodynamic effects, that are equally relevant.

Turbidity currents are sediment-laden flows that are capable of transporting across the continental shelf large amounts of sediments that are finally deposited on the submarine plains. A turbidity current is episodically generated when a significant amount of suspended sediments, either debouched into the coastal region by sediment-laden river outflows, or mobilized by intense sea storms, submarine landslides or earthquakes, reaches the inlet of channels incised through submarine hillslopes (figure 1.19).

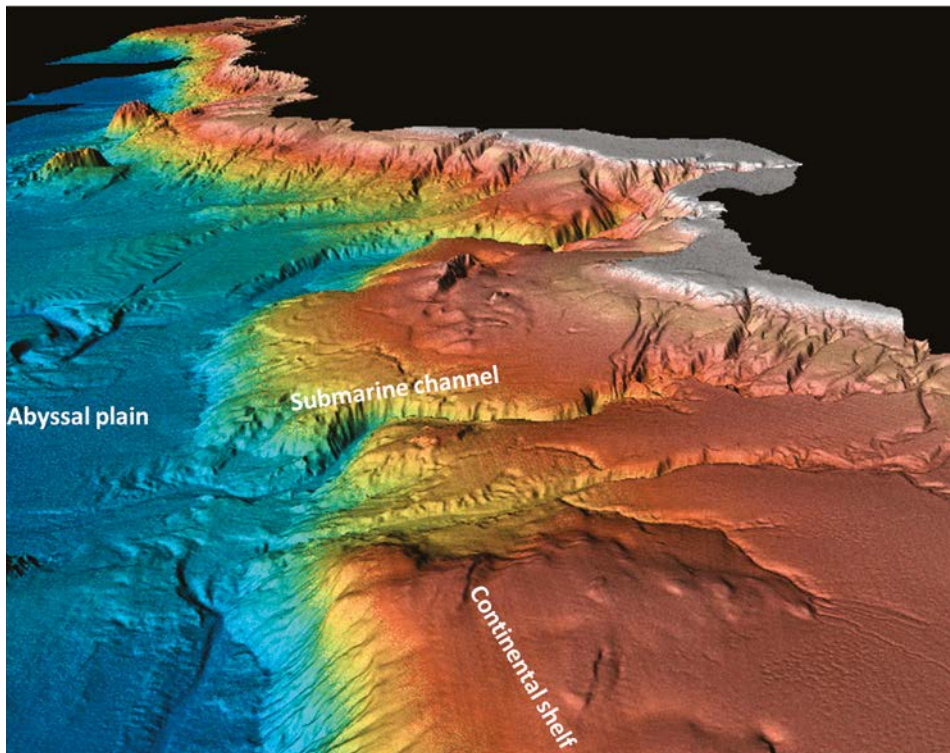


Figure 1.19: The submarine continental shelf off the coast of California, USA, showing channel incisions and the abyssal plain (courtesy Lincoln Pratson).

The water-sediment mixture has a density higher than that of the surrounding undisturbed water. Hence, it moves downslope driven by gravity. As the mixture flows, turbulence is generated and turbulent vortex structures stir up and entrain further sediments from the bottom, thus increasing the density of the mixture. The current then accelerates and increases its transport capacity. This is a self-exciting mechanism that ends when the current encounters the break in slope associated with the transition from the incised channel to the flatter abyssal plain: here, the flow decelerates and the sediments settle generating sedimentary deposits that, in geologic times, evolve into the well known rocks called *turbidites*.

It is quite difficult to perform field measurements of sediment concentration and grain size characteristics, because of the disruptive nature of these currents, which makes it difficult for the instrumentation to withstand the propagation of the front of the current. However, recently Xu et al. (2014) were able to carry out field measurements of the characteristics of the sediment transported by turbidity currents. In particular Xu et al. (2014) analysed the grain size distribution of sediment trap samples collected along the Monterey Canyon after a turbidity current event had taken place. Data refer to various longitudinal coordinates along the channel and vertical distances from the bottom. The measurements clearly show that turbidity currents transport a coarser fraction consisting mainly of very fine sand as well as a finer fraction consisting of a mixture of silt and clay. Moreover, the analysis of coring data taken from submarine canyons and submarine fans shows that the mean grain size of sediment deposited by turbidity currents decreases laterally and longitudinally.

However, accurate information on the spatial and temporal variations of sediment concentration and grain size distribution of turbidity currents can be gained only by means of accurate laboratory measurements. The experimental data confirm that the coarser fraction of the sediments transported by a turbidity current is found at its head and both the sediment concentration and the grain size decrease in the vertical direction and, laterally, away from the bulk of the current where the silt and clay fractions prevail on the fine sand fraction.

Chapter 2

Wandering through our sedimentary world: sedimentary patterns

The sedimentary patterns investigated in the planned series of monographs are generated by the interaction of water with cohesionless or cohesive boundaries in the variety of environments mentioned in Section 1.2. Below, we first discuss what paradigms may help us organize rationally field observations of sedimentary patterns. Next, we employ the above paradigms to introduce the reader to the large variety of patterns encountered in nature.

2.1 Various paradigms to organize field observations

It is preliminarily useful to outline the fundamental general mechanism underlying the formation of sedimentary patterns. Essentially, the amount of sediment that a fluid in motion is able to transport, i.e. its *transport capacity*, depends on the motion intensity and on the characteristics of the available sediments. Hence, a clear fluid subject to a sufficiently intense motion acting over a cohesionless bed progressively erodes the bed by entraining particles until its transport capacity is fulfilled: as soon as this condition is satisfied, the fluid is unable to entrain further sediments or, following a slightly different viewpoint, *the amount of sediments carried by the stream equals its transport capacity*. Conversely, whenever the latter condition is not satisfied, the fluid stream either loses sediments (*deposition*) or gains sediments (*erosion*): the formation of patterns is the response of the sediment interface to spatial-temporal fluctuations of the sediment supply and/or of the transport capacity of the stream, such to generate an unbalance between the two.

Hence, a first paradigm helpful to organize field observations in sedimentary environments is the fundamental distinction between erosional, depositional or quasi-equilibrium patterns: they are respectively characterized by prevailing erosion, prevailing deposition or rhythmic (temporal-spatial) os-

cillations of erosion and deposition such to maintain a spatial-temporal equilibrium.

Various other paradigms, in particular the key concept of spatial and temporal scales of sedimentary patterns, prove helpful. The scale of patterns depends on the physical mechanisms that drive the fluctuations of sediment supply and transport capacity which cause pattern development. Patterns of different spatial (and temporal) scales may coexist, but it will appear that the investigation of patterns of different scales typically requires distinct modeling tools, in particular distinct spatially and temporally averaged descriptions of flow and sediment transport.

A third important and useful paradigm, is the distinction between free and forced patterns. The former arise spontaneously, from instabilities of the liquid-solid interface in the form of interfacial waves affecting the mobile boundary: bedforms and planforms are most often expressions of a free response. Spatial and temporal scales of free patterns are intrinsically chosen by the instability mechanism. On the other hand, erosional and depositional patterns are forced by (typically geometric) constraints imposed at the boundary of the region under consideration. Examples in fluvial environments are an abrupt or progressive reduction of bed slope, channel widening or narrowing, variations of flow rate and/or sediment supply. Examples in the coastal environment are spits (see figure 2.1), tombolos (see figure 2.2) and sand deposits caused by groynes (see figure 2.3). Spatial and temporal scales of forced patterns are associated with the forcing mechanism: e.g. channel widening will produce a pattern the longitudinal scale of which is determined by the widening length.



Figure 2.1: The spit at 'Laghetti di Tindari' (Sicily, Italy) (courtesy of Enrica Calandro).



Figure 2.2: Example of tombolo (Sestri Levante, Italy) (courtesy of Luca De Angelis, official web site: <http://www.lucadea.com/europa/italia/liguria/sestri-levante/>).



Figure 2.3: Groynes at Cavi di Lavagna (Italy) (adapted from Google Maps).

A last useful criterion of pattern classification, can be based on which characteristic of the boundary is affected by pattern formation. The expression of the class of patterns called bedforms is a (possibly migrating) perturbation of *bed elevation*: bedforms typically arise either from an instability of the bed interface or from external geometrical constraints. Typical examples of bedforms are sea ripples and river dunes. Similarly, the straight alignment of fluvial channels is typically unstable to plan form perturbations arising from a complex interaction between outer bank erosion and inner bank deposition. As a result, plan form patterns develop, either building up channel sinuosity (*meandering*) or generating

an interconnected network of curved channels (*braiding* and *anastomosing*). The coastline may also show a sinuous development due to the presence of planform patterns such as beach cusps and longshore crescentic forms that are caused by the interaction of the coastline and the nearshore hydrodynamics. Similar phenomena are observed in transitional environments like coastal lagoons. Finally, so called sorting patterns may be recognized in the spatial arrangement of the grain size distribution of poorly sorted sediment mixtures: their expression is the development of stationary or migrating rhythmic sequences of coarser and finer material.

2.2 Hillslope patterns

Ridge and valley topography exhibiting a distinct characteristic wavelength is the large scale pattern typically observed in soil-mantled landscapes. In this case, the transport capacity of the overland flow induced by precipitations exceeds the sediment supply and erosional patterns develop with rhythmic sequences of hillslope incisions (figure 2.4a). Ridge and valley topography can be described as a *large scale, erosional, forced* pattern. Most sediments delivered through hillslope incisions are deposited at the base of the eroding gully, deposition being forced by the marked break in slope which induces an abrupt decrease in the transport capacity of runoff waters. Sediments accumulate typically in the form of cone shaped bodies called alluvial fans (figure 2.4b). Hence, alluvial fans are *large scale, forced, depositional* features. They tend to be coarse-grained, especially at their mouths but at their edges they can be relatively fine-grained: hence, a *sorting* pattern also develops over the fan.

2.3 Fluvial patterns

In the absence of anthropogenic constraints (e.g. levees), rivers intermittently inundate their adjacent flood plains. Part of the sediments reaching the river network is thus exchanged with the valley where suspended particles settle, progressively building up the flood-plain. Sedimentation overloads the underlain sediment layers, which are then subject to *compaction*. In geologic times compaction leads to *lithification* and the formation of *sedimentary rocks*.

Throughout the whole channel system, the stream continuously undergoes spatial and temporal fluctuations of sediment supply and variations of transport capacity forced by geometrical constraints (channel widening, channel curvature, confluences, bifurcations, variations of channel slope). This leads to diffused pro-

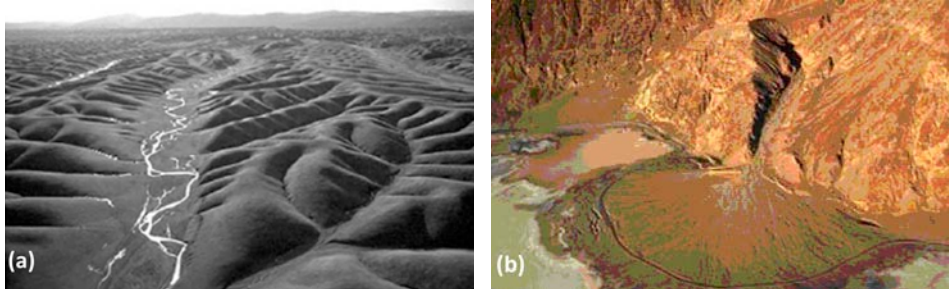


Figure 2.4: (a) Dissected surface of Stony Creek fan, near Orland, California: an erosional forced pattern characterized by rhythmic sequences of valleys spaced roughly 100 m apart. Aerial photograph by James Kirchner (UC Berkeley and ETH Zurich), used by permission; (b) Alluvial fan as a typical example of depositional forced pattern Source: <http://pages.uoregon.edu/millerm/fan.html>, Author Martin Miller.

cesses of erosion and deposition which determine the altimetric and plan form development of the river network. Various fluvial patterns are expressions of this process.

2.3.1 Free fluvial patterns: free bedforms

River beds are seldom plane. Most often, their shape is perturbed by free bedforms, fairly regular oscillations of bed elevation which have the nature of interfacial waves arising spontaneously from an instability of the bed interface: they usually migrate (most often downstream, more rarely upstream) though stationary waves are also observed.

Dunes and ripples.

Dunes are fairly common small scale bedforms with typical wavelengths scaling with flow depth and amplitudes of the order of a fraction of flow depth. Dunes migrate invariably downstream.

Their shape displays a strong asymmetry, marked by the presence of fairly sharp fronts. The shape of fronts observed in nature (figure 2.5 bottom) is often three-dimensional though 2-D dunes have been observed in the laboratory and have extensively been studied theoretically. It has been ascertained that, as the flow gets shallower, 2-D configurations lose stability to 3-D oblique configurations. Note that, under steady conditions dunes reach a state of equilibrium: in other words, in a spatially averaged sense, they are neither erosional nor depositional features. Dunes are typically observed in sandy streams, but very low amplitude dunes have also been detected in gravel bed rivers. Smaller bedforms (ripples), quite similar to dunes, are observed when the turbulent stream flows in

a hydraulically smooth or transitional regime, which most often is also associated with weak sediment transport. These forms are less strongly asymmetrical than dunes and migrate downstream (figure 2.5 top).

Antidunes and cyclic steps.

A distinct class of small scale bedforms scaling with flow depth is observed in supercritical streams: they are called antidunes and, unlike dunes, they are quite symmetrical and may migrate either downstream or upstream (figure 2.6). When the flow is near critical conditions antidunes do no longer migrate and turn into so called stationary waves. Similarly to antidunes, cyclic steps are bedforms that develop in supercritical streams though, when the cyclic step has grown, the flow does no longer maintain its supercritical character along the whole bedform length and a hydraulic jump forms (figure 2.7). Moreover, unlike antidunes, cyclic steps are 'long' waves with wavelengths much larger than flow depth and are fairly 'stable' wave trains which preserve their pattern while migrating upstream.

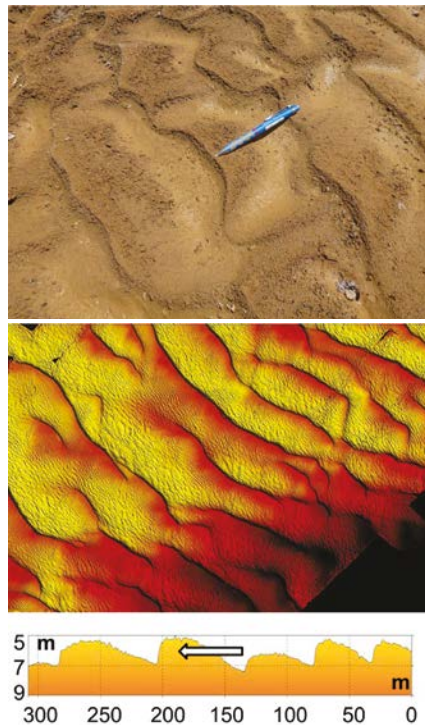


Figure 2.5: Top: Current ripples seen in plan view. Flow from right to left (Source: <http://stratiland.files.wordpress.com/2013/05/2.jpg>). Bottom: Dunes in the Parana River (Parsons et al., 2005). Note the 3-D shape of fronts and the presence of smaller scale bedforms superimposed on the large 3-D dunes. Inset: bed profile following the line indicated on the 3-D image (courtesy of Jim Best).

Longitudinal bedforms: sand ridges.

Bedforms displaying fronts parallel to the stream are also observed: they are called sand ridges and are stationary bedforms. They are intrinsically associated with the formation of secondary flow cells aligned with the channel axis and driven by turbulence anisotropy (Colombini (1993)). Sediments are then displaced in the lateral direction building up some lateral slope until the destabilizing effect of the secondary flow, that tends to accumulate sediments over the crests, is balanced by the stabilizing effect of gravity, that acts to let sediments move downslope towards the troughs.



Figure 2.6: Strongly 3-D current antidunes on a creek, located in Urdaibai estuary (Basque Country) (Source: Wikimedia Commons, the free media repository).

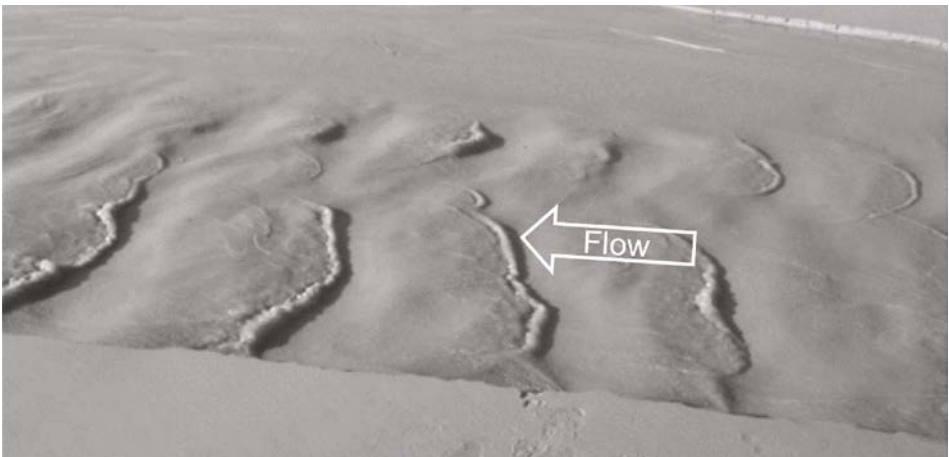


Figure 2.7: Cyclic steps observed on a beach near Calais (France). Photo by and courtesy of H. Capart. The bedforms did not display a clear direction of migration (Capart, personal communication).

Fluvial free bars.

At a larger scale, river beds display an important class of rhythmic perturbations of bed elevation called bars. Their distinct feature is that they are organized in rows of periodic sequences of riffles and pools separated by oblique fronts. The number of rows displayed by the pattern depends on the channel width. Very narrow channels do not allow for bar formation, in fairly narrow channels a single

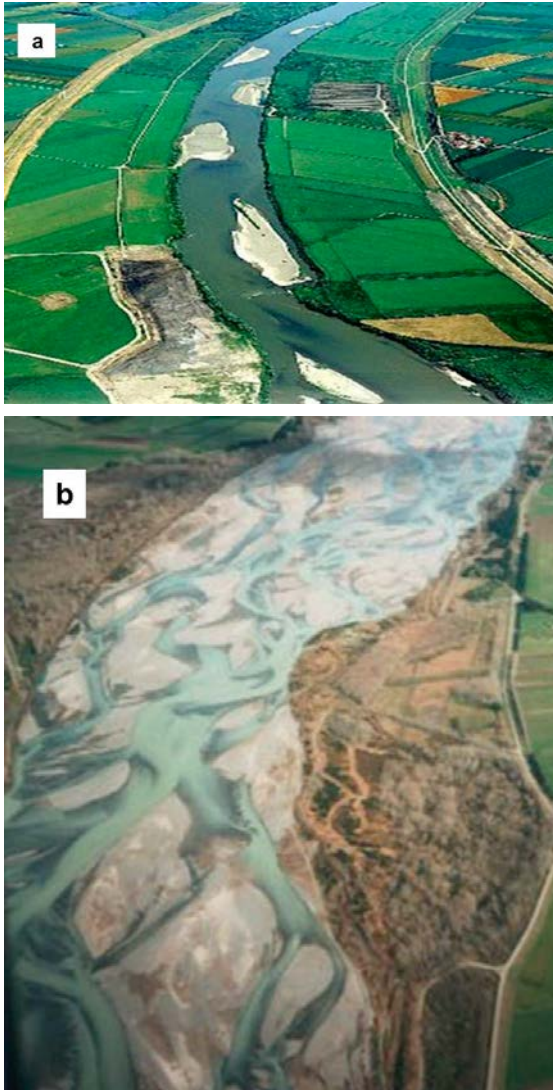


Figure 2.8: (a) Tokachi River, Japan. The flow is from top to bottom. Photo Hokkaido Development Bureau (courtesy of Y. Shimizu). (b) Multiple row bars in the braided Waikariri River, New Zealand (courtesy of Bianca Federici).

row pattern (alternate bars) is observed (figure 2.8a) whereas multiple row patterns form in wide channels (figure 2.8b). Note that both single and multiple row bars are large scale migrating features.

As discussed below, single row patterns are observed in straight or weakly meandering rivers, whilst multiple row patterns are typical of so called braided rivers.

Sorting patterns: bedload sheets and longitudinal streaks.

As pointed out by Seminara (1995), some fluvial bedforms are generated or dominantly controlled by grain sorting. They are bedload sheets and longitudinal streaks.

Bedload sheets are smallest dune-type transverse bedforms observed in gravel bed rivers. They have the nature of sorting patterns being characterized by a rhythmic sequence of coarse and fine material. Their amplitudes are very low (of the order of few grain sizes) and they migrate downstream (figure 2.9a).

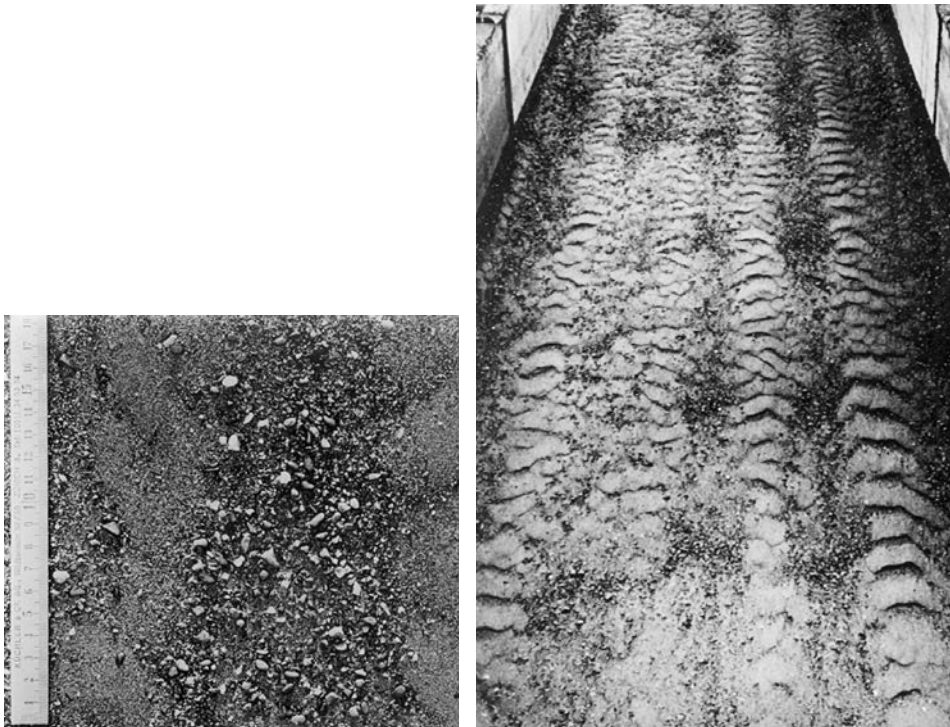


Figure 2.9: (a) Bedload sheets observed in the laboratory (Whiting et al., 1988) (b) Longitudinal streaks with ripples superimposed on the fine streaks. Flow is from bottom to top (Colombini and Parker, 1995). Original photograph from Günter (1971).

If the sediment is heterogeneous, longitudinal bedforms similar to sand ridges still form. However, they display distinct features arising from an independent sorting mechanism whereby finer (coarser) material accumulates in the crests (troughs) of the ridges. They are called longitudinal streaks (figure 2.9b).

Unlike in the case of bedloadsheets and longitudinal streaks, most other bedforms (river dunes, free and forced fluvial bars) are moderately affected by sorting which is invariably found to lead to a damping effect on bedform growth.

2.3.2 Forced fluvial patterns

Forced fluvial patterns arise typically (but not only) in response to prescribed variations of channel geometry. Some examples are illustrated below.

Channel widening is often associated with the formation of a central bar, which is the precursor of a river island (figure 2.10). Channel curvature is responsible



Figure 2.10: Central bar associated with channel widening close to the confluence of Alatna and Koyukuk Rivers, Alaska (Source: <https://upload.wikimedia.org/wikipedia/commons/thumb/9/98/Alatna.jpg/400px-Alatna.jpg>).

for the generation of the so called *point bars* (figure 2.11), accumulations of sediments along the inner bends of meandering rivers whereby the thread of high velocity of the stream is shifted towards the outer and deeper part of the bend. Figure 2.12 shows the so called *scroll bars*, which record the various steps of the process of lateral migration of meander loops. Steady bars are sometimes observed upstream of channel reaches undergoing geometrical variations, e.g.



Figure 2.11: Point bars forced by curvature in a sequence of meanders of the Po River near Cremona (Italy) (<http://www.parmaitaly.com/foto/Po-secca-lug2015-2.jpg>).



Figure 2.12: Scroll bars record the various steps of the process of lateral migration of meander loops: an example from the Ob River, Siberia (http://www.seddepeq.co.uk/depositional_env/fluvial/meander/meander.htm).

bifurcations (figure 2.13a) or the transition between a straight and a curved reach (figure 2.13b). In the latter case, steady bars are invariably present downstream of the bend though upstream bars may also be generated when the channel is fairly wide (figure 2.13b). This is a process whereby morphodynamics gives rise to an upstream influence that would not occur under fixed bed conditions.

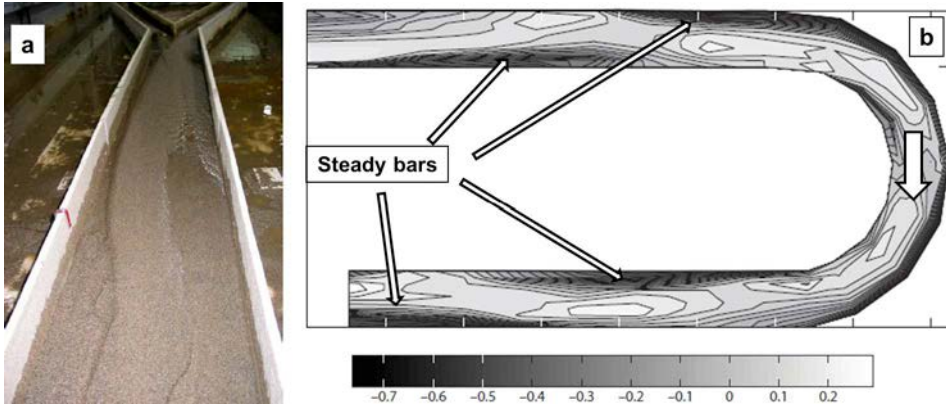


Figure 2.13: (a) Steady bar forced upstream of a channel bifurcation (Courtesy of W. Bertoldi) (b) Steady bars forced upstream and downstream of a channel bend (modified from Zolezzi et al. (2005), figure 14).

2.3.3 Fluvial planforms

As already mentioned, the floodplain is continuously reworked through sediment exchange with the river network. Sediment is lost by the floodplain to the river as a result of bank erosion; removal and deposition of part of the collapsed material, later consolidated by vegetation leads to floodplain reconstruction.

River meandering

The most fascinating of these patterns is river meandering.

Bank erosion, enhanced by fluctuations of the flow discharge, shifts outward the channel axis *producing curvature*, while inner bend deposition tends to keep the river width fairly constant. As a result, the channel centerline wanders through the flood plain generating a variety of patterns, the striking feature of which is their regularity. Then, it is not surprising that the origin of river meandering attracted the attention of great scientists, most notably Albert Einstein (Einstein, 1926).

The evolution of meandering rivers in nature undergoes a number of cyclic events. At their juvenile stage, meanders are weakly curved and coexist with mi-

grating alternate bars (figure 2.14). As the outer bank erosion progresses, meanders amplify and migrate typically downstream. Amplification eventually leads adjacent branches of a meander loop to approach each other, to the extent that the stream undergoes a so called *neck cutoff* and the abandoned loop becomes an 'oxbow lake' (figure 2.15b). In other cases chutes are formed by lateral erosion



Figure 2.14: Meandering rivers observed in the field display a variety of patterns. The Alutna River meanders south from the Gates of the Arctic National Park and Preserve, Alaska. Note the juvenile meanders developing after the old meanders on the right have undergone cutoff, with the abandoned meanders turning into oxbow lakes (Source: <https://www.terrageria.com/images/np-alaska/gaar0023.jpeg>).

of the bank of the upstream arm of a loop, which causes the stream to cut through the neck of the loop into the downstream arm (figure 2.15c). High-gradient chutes may eventually divert the stream, again leaving the former loop as an isolated oxbow lake.

Finally note that meanders typically form in alluvial valleys but they are also observed in rocky environments, where they develop spectacular landscapes (figure 2.16).

River braiding

An equally fascinating plan form pattern is observed in wide rivers. The stream of *braided rivers* splits into a network of small channels (*braids*) separated by typically migrating bars, which may turn into fixed or temporary islands (2.17b). Both channels and bars are typically highly mobile during flood events, such that details of the pattern may undergo significant changes after the flood.

Note that a variant of braided rivers are the so called *anastomosing rivers* which also display a network of interconnected channels. The distinct feature of anastomosing rivers is, however, the character of channels which have low gradient, are narrow, deep and characterized by stable banks (2.17a).



Figure 2.15: (b) Meander of the Alatna River in the process of being cut off (Source: www.politicalstew.com). (c) A reach of the William River (U.S.A.) displaying a sequence of chute cutoffs (Source: <https://s-media-cacheak0.pinimg.com/564x/86/e8/89/86e889b7a937503b053132b331d65caa.jpg>). Photo by N. D. Smith).

2.3.4 Fluvial patterns and river engineering

River engineering deals with the technical problems arising in the various activities related to the exploitation of river basins. Any such activity, in a way or another, affects river morphology and is influenced by the erodible character of the channel boundary. A few examples may help clarifying the latter statement.

Damming of river basins has been a common practice throughout the last century for a variety of purposes, including energy production, water supply, irrigation, flood protection and recreational purposes. The important role played by reservoirs in promoting development cannot be underrated. This notwithstanding, river damming exhibits major shortcomings as dams, besides storing water, interrupt sediment transport: part of the sediment load settles within the reservoir leading to some undesirable effects. Firstly, the available storage volume is progressively reduced. Removing sediment deposits from dam reservoirs is a costly action, the more so if sediments are polluted and require some treatment to be disposed. Secondly, the sediment load carried by the stream is severely cut downstream, leading to bed degradation and armoring phenomena. In the worst cases, as discussed in Section 2.4.3, problems may even extend down to the delta region which may suffer for accelerated subsidence phenomena. Early reviews of the geomorphological effects of damming are found in Galay (1983) and Williams



Figure 2.16: An example of meandering in rocks: the sinuous course of the San Juan River (Goosenecks State Park, Utah) cuts deep into the sandstone (Source: earthobservatory.nasa.gov).

and Wolman (1984). For a more recent assessment see Garcia (2008), Chapters 1 and 12.

Straightening of meandering rivers has also been often pursued in order to increase the conveyance of river reaches and promote navigation. A major example was the sequence of 14 artificial cutoffs constructed by the US Army Corps of Engineers between 1929 and 1942, in the lower Mississippi River between Mem-



Figure 2.17: (a) The braided Bramaputra River in the vicinity of Arunachal Pradesh, India. (Source: Google Maps) (b) A reach of the Columbia River an anastomosing river of British Columbia, Canada (Photo by H.J.A. Berendsen).

phis, Tennessee, and Red River Landing, Louisiana (figure 2.18). This type of intervention has major effects. Firstly, a net shortening of the river: approximately a 235 km reduction in the Mississippi case mentioned above (Winkley, 1977). This makes the river more efficient for navigation. Moreover, the increased slope in the straightened reach generates typically a degradation wave propagating upstream and a depositional wave migrating downstream. Adjustment of the bed profile occurs on a quite long time scale (of the order of decades) and may affect severely the stability of banks and river infra-structures.

Sand mining from river beds has also been a common practice in the last century. Its major morphological effect is river degradation. An example of such phenomena is depicted in figure 2.19 showing the severe degradation undergone by the Magra River (Tuscany, Italy) that had been used as a sand-gravel mine for the construction of an important highway in the 1950's. Bed degradation is a source of risk of failure of river infrastructures. Figure 2.20 shows an example of potential bridge failure caused by the propagation of an erosion wave along the bed of the Tanaro River (Italy).

Modifications of the river morphology for practical purposes are sometimes sought through the construction of appropriate structures. *Dikes* are a typical ex-

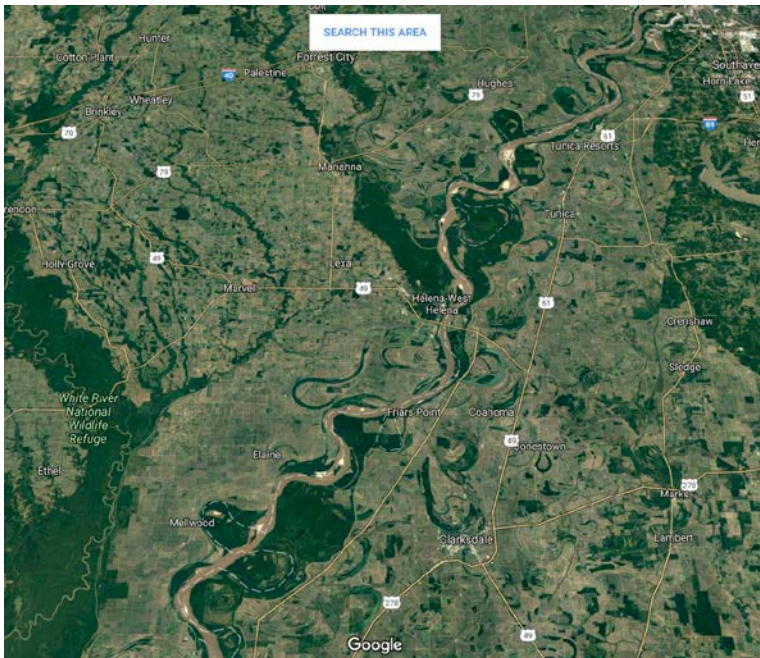


Figure 2.18: A satellite view of a reach of the Mississippi river downstream of Memphis (Tennessee). Note the several oxbow lakes formed after artificial and natural cutoffs (Google Maps).

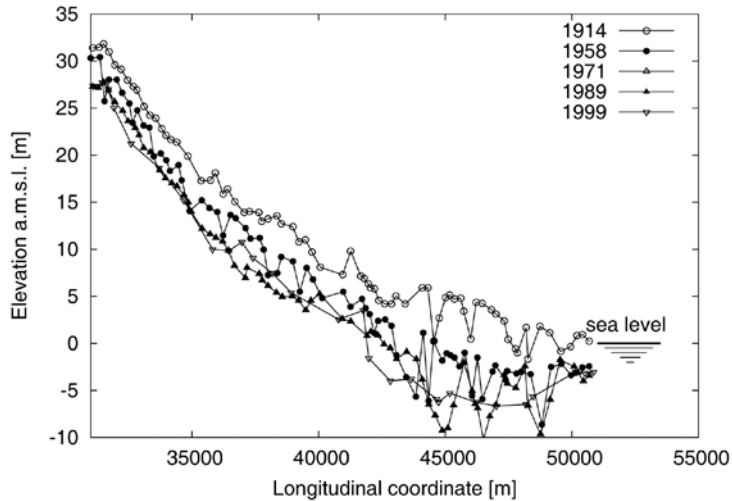


Figure 2.19: Degradation of the terminal reach of the Magra river (Tuscany, Italy) driven by an excessive extraction of bed material in the 1950s for the construction of an important highway (Adapted from Rinaldi (2005)).



Figure 2.20: Bed degradation of the Tanaro River (Piedmont, Italy) at Barbaresco-Molini d'Isola d'Asti has given rise to the severe erosion of the bridge piers (Seminara et al. (2003)).

ample: their function is to reduce the 'effective width' of the river, deepening the channel such to allow for navigation. Dikes have been widely employed in most major rivers throughout the world. Figure 2.21 shows a sequence of pictures illustrating the morphological impact of the construction of dikes in a reach of the



Figure 2.21: The progressive siltation of a dike system, Indian Cave Bend, Missouri River. (a) September, 1934 (before construction); (b) November, 1934 (just after construction); (c) August, 1936; (d) May, 1946 (Reproduced from Alexander et al. (2012)). Credit: U.S. Geological Survey. Department of the Interior/USGS.

Missouri River. Impacts on river (and floodplain) morphology are induced by any river infrastructure. *Levees*, preventing the inundation and sediment settling in the floodplain, promote aggradation and a tendency of the river to become pensile (figure 2.22). They also prevent bank erosion, thus suppressing the bank contribution to sediment transport, and constrain meandering rivers that are no longer allowed to undergo plan form development.

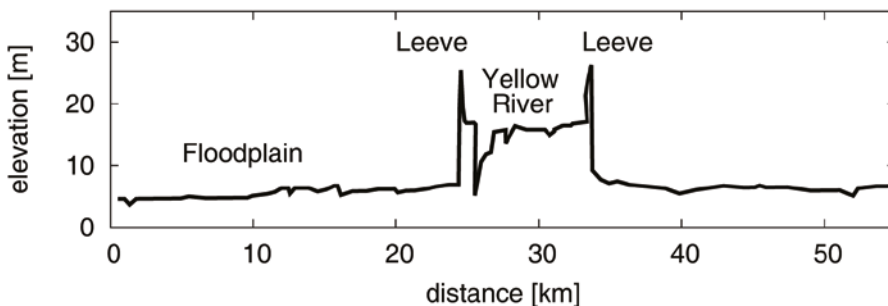


Figure 2.22: The Yellow River is pensile in its terminal reach: note the levee height, that reaches about 20 m, and the average bed elevation that is much higher than the elevation of the floodplain (adapted from Yisan and Fuling (1989)).

Diversions of part of the river discharge for any purpose (water supply, energy, irrigation, flood protection) also affects the river morphology as, downstream of the diversion, the solid discharge of the river is reduced and differs from the modified transport capacity of the fluvial stream.

Infrastructures also interact with *erosional-depositional waves* associated with natural processes (e.g. bedform migration or flood propagation). For example, bridge piers in erodible beds are subject to erosional mechanisms driven by flow perturbations. If migrating bedforms (dunes, bars) are present, then bridge scours is significantly enhanced.

Finally, predicting the occurrence, modeling the propagation and preventing the catastrophic impact of debris and mud flows are major issues, not fully settled yet, that will deserve an assessment through a specific monograph of the present series.

2.4 Transitional patterns

2.4.1 Transitional plan forms

As mentioned above, one of the distinct features of transitional environments is the fact that the flow field and sediment transport, besides feeling the effect of the fluvial stream, are also affected by tides, winds and waves.

Deltas

River deltas are the fundamental transitional geomorphic features where the coexistence of the above effects is displayed through a variety of spectacular patterns. The 'size' of deltas is naturally correlated with the extension of the river watershed, ranging from few square kilometers for small rivers to tens of thousands of square kilometers: the Amazon delta, the largest river delta in the world, extends over 467,000 km² (Syvitski and Saito, 2007).

River deltas are depositional features: they form whenever the fluvial stream carries enough sediment and the hydrodynamic control imposed by the ocean leads to a transitional flow field characterized by a transport capacity decreasing downstream. Hence, the tidal forcing cannot be too strong: if tidal currents prevail, then sediments are advected away from the inlet and the river forms an *estuary* rather than a delta.

It has been suggested (Galloway, 1975) that a general paradigm to interpret the morphology of river deltas is the relative roles played by the fluvial stream, the wave climate and the tide. This is illustrated in the ternary diagram of figure 2.23.

When the *role of tides and wave action is low*, delta formation is controlled by

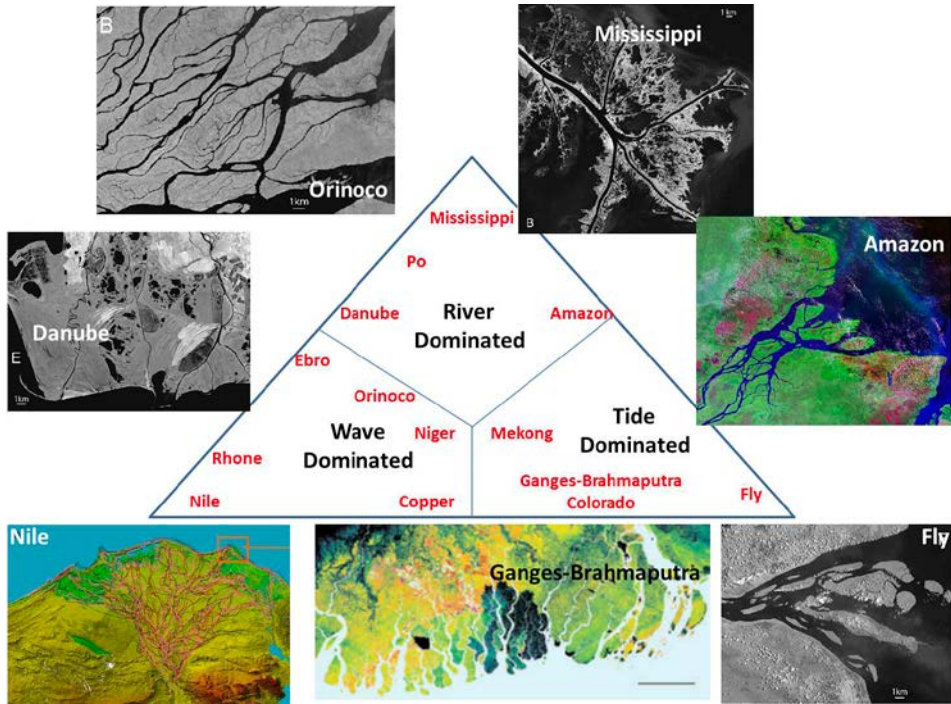


Figure 2.23: Sketch illustrating the various controls on deltas and the different patterns observed (modified from Galloway (1975)).

the process called *avulsion*. Slope reduction is the cause of avulsions. The original river course becomes unstable to one (or many) hydraulically more efficient paths to the ocean: during floods, the fluvial stream may breach its natural levees and cut a new channel characterized by a route to the ocean with slope higher than that of the original channel. This process is also promoted by bed aggradation in the original channel, which makes it easier for the stream to breach its natural levees. Avulsions do not necessarily deviate the whole flow into the new channel, but may simply give rise to a bifurcation. Delta networks develop as the occurrence of such bifurcation events repeats systematically. Avulsion, however, is not the only mechanism whereby delta networks in low marine energy environments may develop. An alternative mechanism is the formation of bars at the river mouth, where sudden deceleration leads to sediment deposition. A central bar is the precursor of a bifurcation as it forces the stream to flow around it, eventually splitting the original channel into two distinct channels.

Deltas where the *tidal amplitude is high* are characterized by funnel shaped channels: the cross section of these channels is controlled by the so called *tidal prism*, namely the tidally driven volume of water exchanged with the sea in half a tidal cycle. As the tidal prism increases relative to the fluvial contribution, funneling becomes more pronounced (Figure 2.26).



Figure 2.26: The tide dominated delta of the Niger river (Google Maps).

Estuaries

Estuaries are morphological features observed when a river meets a macrotidal coastal environment and the tidal forcing largely exceeds the fluvial forcing. This simple definition is strictly related to the etymology of the word estuary, that goes back to the Latin word *aestus* which means tide. Just like in tidal dominated deltas the distinct feature of estuaries is their funnel shape (Figure 2.27).



Figure 2.27: The Delaware estuary (a) and the Gironde estuary (b) (Google Maps).

Lagoons

A different, albeit related, transitional pattern forms when a typically elongated portion of the coast transforms into a shallow water body separated from the sea by barrier islands. These water bodies are called *lagoons*, a word derived from the Italian word *laguna* referring to the Lagoon of Venice. Coastal lagoons are typically connected to the sea through fairly narrow channels separating the barrier islands, which are called *inlets*. Also, a variety of lagoons exists with various degrees of salinity, depending on the number of inlets, the amplitude of tides and the amount of inflow of fresh water.

In general, the morphological structures composing a lagoon consist of *barrier islands*, *inlets*, *channel network*, *shoals* (regions permanently submerged adjacent to tidal channels) and *salt marshes* (regions periodically inundated by tidal currents where halophytic vegetation grows) (figure 2.28).

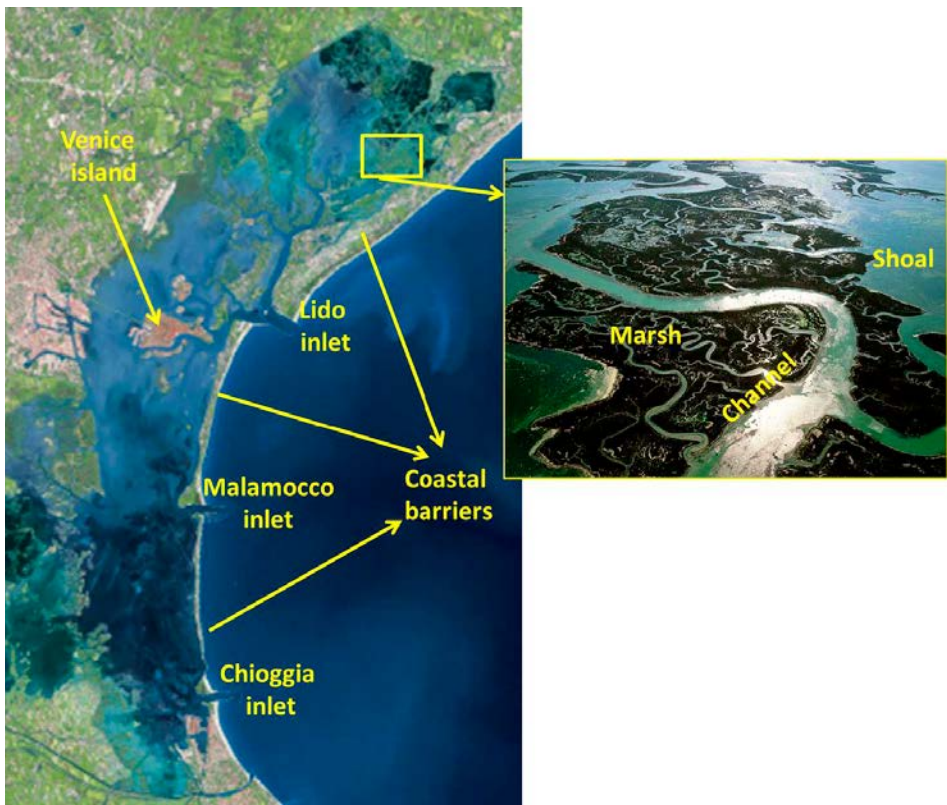


Figure 2.28: The morphological structure of Venice lagoon.

2.4.2 Transitional bedforms

Large and small scale bedforms, both free and forced, are observed also in transitional environments, though the available literature on the subject is less extensive than in the fluvial case (Dalrymple and Rhodes, 1995). Transitional bedforms include ripples and dunes (figure 2.29), free and forced bars (figure 2.30). Most often, channels meander (figure 2.28) and display most of the evolutionary features described by fluvial meanders, including neck cutoffs, albeit their development is typically slower than in the fluvial case.



Figure 2.29: Dunes exposed at low tide along the margin of Pats bar in the Columbia River Estuary (Image courtesy of the TIFZ project, www.brighton.ac.uk/columbia).



Figure 2.30: Free and forced tidal bars observed in tidal channels at Skallingen, Denmark (Google Maps).

2.4.3 The impact of development on transitional environments.

Today, more than 500 million people live in coastal regions within 5 m of sea level, in areas that occupy just 1% of the Earth's land surface. Indeed, transitional environments, i.e. river deltas, estuaries and coastal lagoons, have played a major role in the course of human development. Deltas have historically attracted the establishment of human settlements from which some of the great civilizations originated. Settlements have increased at a rate that has exploded in the last half century. They are favored by the characteristics of deltas, typically flat regions with average slopes smaller than 10^{-5} , with soils rich in nutrients and ideal for farming rice and other crops. Deltas are also typically dissected by a network of waterways which allow for easy access to oceans and make them ideal settings for commercial hubs. Finally, deltas are also typically huge gas/oil reservoirs that have been largely exploited in the last century and will likely continue to be exploited in the near future.

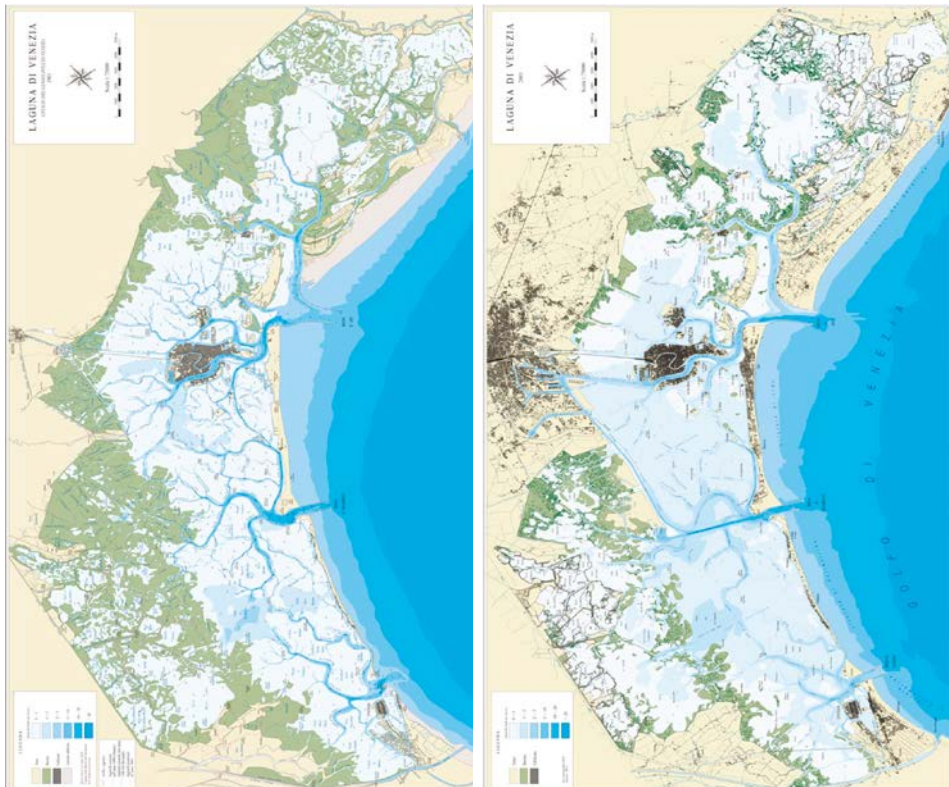


Figure 2.31: Comparison between the morphological structures of Venice lagoon in surveys of 1901 (left panel) and 2003 (right panel). Salt marshes are the green areas (courtesy of L. D'Alpaos).

On the other hand, natural deltas and coastal lagoons (that occupy 13% of the coastal regions of the world) are environments of special ecological value, rich of biodiversity, that would deserve to be carefully preserved. However, as a result of a variety of both natural and anthropogenic effects, in the last century these environments have undergone severe and accelerated degradation that, in some cases, threatens their survival. A major example is the case of Venice lagoon where salt marshes have dramatically reduced their extension throughout the last century and the tidal flats in the central and southern part of the lagoon have deepened so intensely that the lagoon is slowly turning into a bay (figure 2.31).

The main process commonly held responsible for the acceleration of sinking of the coastal regions is eustatic sea level rise. And, indeed, current predictions of sea level rise due to global warming for the present century (figure 2.32) enhance our worries: *"Projections of global average sea level rise from 1990 to 2100, using a range of AOGCMs following the IS92a scenario (including the direct effect of sulphate aerosol emissions), lie in the range 0.11 to 0.77 m"* (Pachauri et al. (2014)). However, besides sea level rise, anthropogenic factors have significantly contributed to the process of sinking deltas.

Subsidence of coastal territories is a major factor. Subsidence is a natural process that has been lately enhanced by various causes. In some areas, e.g. the New Orleans area, soil consists mainly of peat, namely a soil of organic nature that forms in wetlands. Here, residues of vegetation accumulate in stagnant water, where they are unable to oxidize and form peat. The thickness of the peat layer in the New Orleans area is about 5 m. Peat soils, when drained, subside as a result of consolidation (driven by water loss), compaction (the soil porosity decreases

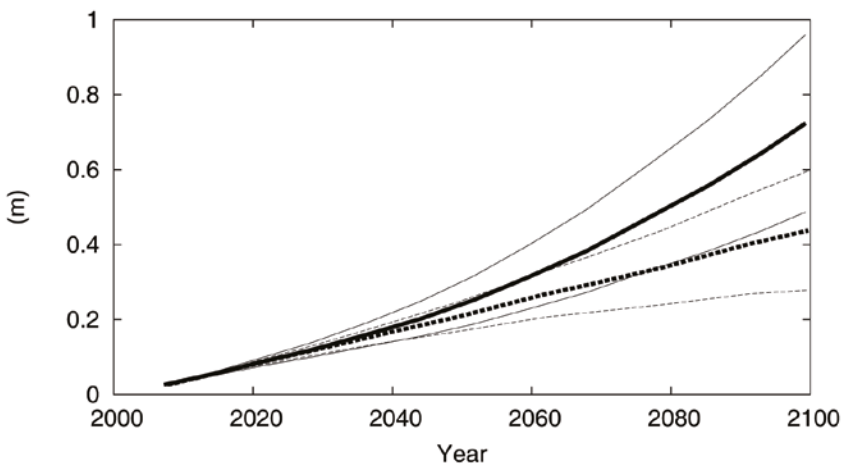


Figure 2.32: Global mean sea level rise from 2006 to 2100 as determined by multi-model simulations. All changes are relative to 1986 - 2005. Time series of projections (thick lines) and a measure of uncertainty (thin lines) are shown for scenarios RCP2.6 (broken lines) and RCP8.5 (continuous lines).

as the soil is loaded) and sublimation (as a result of lowering of the water table, the peat is exposed to the action of air, oxidizes and then sublimates) (Waltham (2005)). A second major cause of subsidence is the intense underground extraction of fluids (water, gas, oil). This applies to most deltas around the world. As an example, the impact of oil industry on the economy of Louisiana is enormous, encompassing thousands of oil and gas pipelines (amounting literally to thousands of kilometers), 5000 offshore platforms, hundreds of thousands jobs. The third major cause of subsidence is the reduced sediment supply to deltaic regions due to regulation works performed throughout river basins, e.g. damming of rivers and their tributaries for flood protection, to prevent summer droughts and provide for hydroelectric energy and recreational assets. In particular, before 1900 the Mississippi River system delivered an annual sediment load around 400 M tonnes to coastal Louisiana: this value has decreased to 145 M tonnes in the period (1987-2006) (Meade and Moody (2010), figure 2.33). Moreover, river channelization and levee construction have prevented the periodic flooding of the delta region, whereby part of the sediment load settled in the floodplain. As a result, in some areas of the Mississippi delta, subsidence has reached local peaks around two meters in a century! A fourth factor has induced subsidence of major Asian river deltas, namely aquaculture, a major industry developed in Asia to meet the growing demand for seafood, in particular shrimp (figure 2.34): 65.6 M tonnes of fish were produced from inland as well as marine aquaculture in Asian countries in 2014, as compared with a total of 11 M tonnes produced in 1990. According to FAO (FAO (2016)), Asian aquaculture accounts for 89% of the world production! It has been recently suggested (Higgins et al. (2013)) that groundwa-

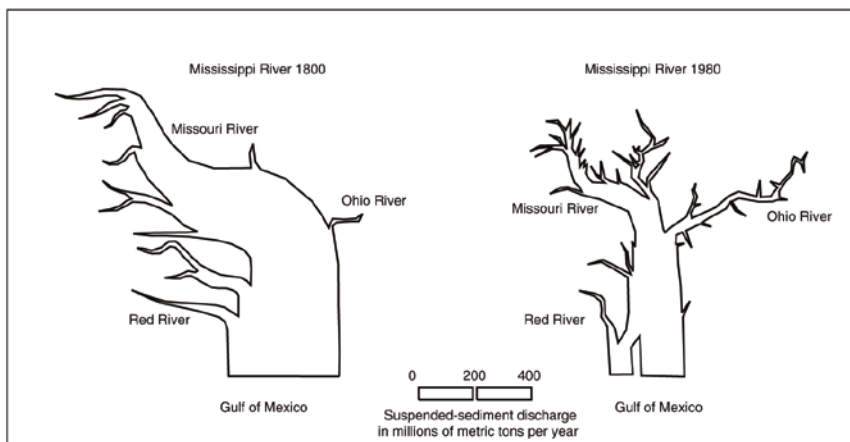


Figure 2.33: The sketch illustrates the reduction of suspended sediment discharge delivered through the Mississippi and its tributaries due to regulation works constructed throughout the Mississippi basin (adapted from Meade and Moody (2010)).



Figure 2.34: A shrimp pond at Cà Mau, in the Mekong delta (Photo by Hong Van for Future Earth, Vãn and Moffett (2014)).

ter extraction at aquaculture facilities induces sinking of the Yellow River delta at a rate (250 mm/y), two orders of magnitude higher than the local and global sea level rise! Moreover, farmers have been replacing mangroves with shrimp ponds: e.g., roughly half the mangrove forest on the Mekong Delta has been cut down for this purpose. This has prevented the important functions of mangroves, namely the production of organic sediments able to build up land and their ability to act as a barrier against the disrupting action of sea storms.

The knowledge made available through the present series of monographs is ultimately also aimed at analyzing the existence of feasible solutions to the major problems created by unsustainable development occurred in transitional regions throughout the last century and continuing in the present century.

2.5 Coastal patterns

The sea bottom and the beach face are shaped by the action of waves and currents, the characteristics of which change in time and space. Hence, the interface between the granular bed and the flowing water changes continuously. This notwithstanding, the pattern attains typically a sort of 'dynamic' equilibrium.

The '*equilibrium profile*' of both the sea bottom and the beach face depends on the characteristics of the actual current and wave climate but it is often characterized by the presence of morphological patterns with a wide range of spatial scales, ranging from a few centimeters to tens of kilometers. Often these forms are repetitive both in space and time. Examples are ripples, megaripples, beach cusps, crescentic forms, sorted bedforms, sand waves and tidal dunes, long bed waves, shoreface-connected ridges and sand banks. They can be classified using the paradigms discussed in Section 2.1. As in the fluvial case, we distinguish bed forms from plan forms, the latter being those patterns which shape the beach face and the coastline. Then, let us describe the morphological patterns observed in coastal regions, proceeding from those characterized by the smallest scales up to those exhibiting the largest features.

2.5.1 Coastal bed-forms

Coastal ripples

Ripples (see figure 2.35) are the smallest periodic bedforms observed in coastal regions. They are generated by the oscillatory flow induced close to the bottom by surface waves propagating into shallow waters and their characteristics are different from those of the ripples generated by steady currents. Indeed, when an oscillatory flow interacts with the bottom undulation of small amplitude generates a steady streaming which consists of recirculating cells. When the steady velocity component close to the bottom is directed from the troughs towards the crests of the bottom undulation, the sediments move from the trough towards the crest. The tendency of the sediments to pile up near the crests is opposed by the component of the gravity force acting in the downslope direction. It follows that the growth of the amplitude of the bottom waviness and the formation of ripples are controlled by a balance between these two effects. On the other hand, due to their (temporally and spatially) slowly varying character, tidal currents drive the formation of ripples similar to fluvial ripples.

Coastal ripples display a symmetric profile, unless a steady current is superimposed on the wave driven oscillatory flow or the wave height is so large that the forward velocity is significantly larger than the backward velocity, such that the symmetry of the oscillatory flow is broken. The wavelength of coastal ripples is comparable to the amplitude of the fluid displacement oscillations induced by the propagating waves close to the bottom [$O(10\text{ cm})$]. Also, these forms have typical amplitudes of a few centimeters. They play a prominent role in the mechanics of coastal sediment transport, since the flow usually separates at the crests of the bed forms and generates vortex structures, that pick-up sediments from the bottom and entrain them into suspension.



Figure 2.35: Ripple marks in the Mediterranean Sea (courtesy of José B. Ruiz).

Typically, sea ripples are quasi *two-dimensional* (see figure 2.35) but *three-dimensional ripples*, either regular or irregular, may also be observed. In particular, depending on flow and sediment characteristics, a type of regular three-dimensional ripples, called *brick-pattern ripples*, was observed mainly in laboratory experiments. Just like for two-dimensional ripples, the crests of these bedforms are perpendicular to the direction of the fluid oscillatory motion. However, the crests of brick-pattern ripples are joined by equally spaced bridges which are parallel to the direction of fluid oscillations.

Bridges are shifted by half a wavelength between adjacent sequences, such that the overall bottom topography resembles a brick wall (figure 2.36).

Other types of three-dimensional regular ripples may form when a complex wavefield is present, e.g. when the wavefield is generated by a monochromatic wave approaching obliquely a coastal structure. Under these conditions the wave is partially reflected: as a result, the velocity close to the bottom is no longer unidirectional and the velocity vector rotates during the wave cycle describing an ellipse. Ripples observed under these conditions are known as *hexagonal or tile ripples*. A photo of hexagonal ripples can be found in Allen (1984).

The ratio h_r / ℓ_r between ripple height and ripple length is usually large enough to cause the separation of the wave driven bottom boundary layer from the bedform crest: ripples formed under these conditions are the so called *vortex ripples* (see figure 2.37). However, in laboratory experiments one observes a different kind of ripples called *rolling grain ripples* (see figure 2.38), characterized by values h_r / ℓ_r smaller than 0.1. Under these conditions, the oscillatory boundary layer keeps attached to the bottom, no vortex is generated and sediments simply roll and slide along the bottom.

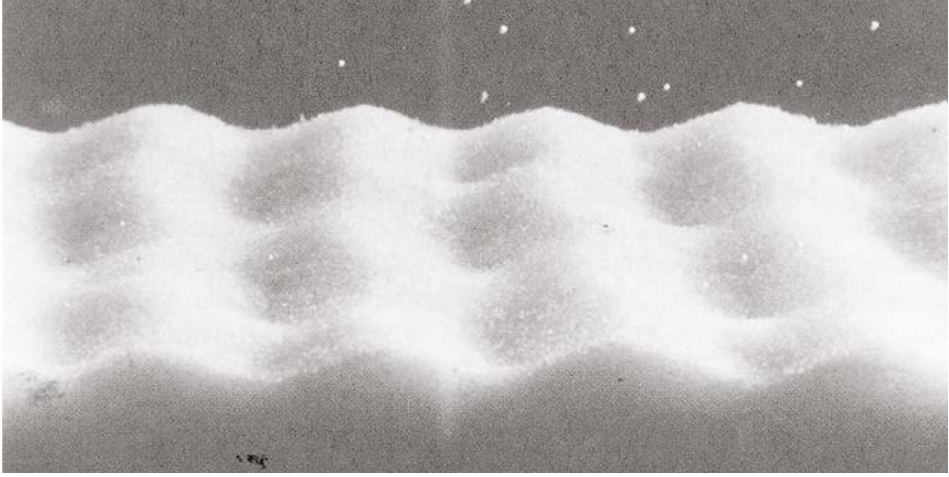


Figure 2.36: Brick-pattern ripples observed during a laboratory experiment (courtesy of John F.A. Sleath).

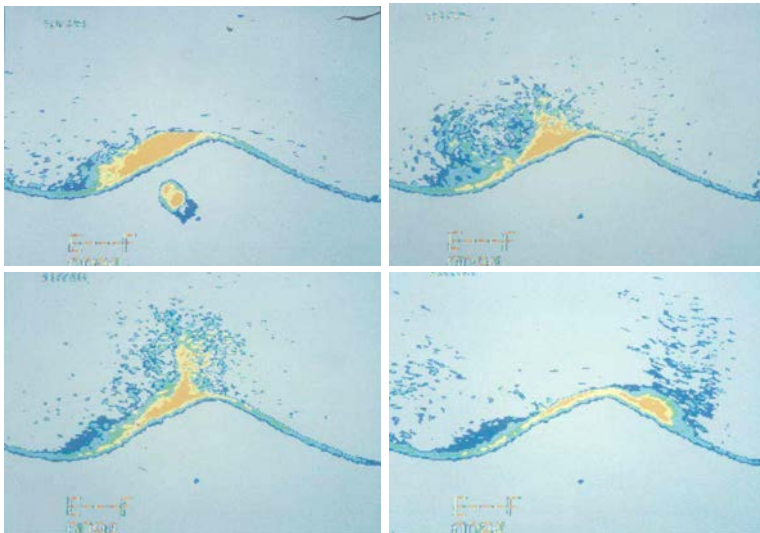


Figure 2.37: Qualitative images of sediment concentration over a vortex ripple at different phases of the oscillatory cycle. Different colors indicate different values of the sediment concentration (Blondeaux and Vittori, 1990).

Megaripples and hummocks

Finally, bedforms of larger size, with wavelengths in the range 1 – 5 m and heights of tens of centimeters, are observed on the shelf (e.g Swift et al., 1983, Van de Meene et al., 1996, Kleinhans et al., 2004), in the surf zone (Greenwood and Sherman, 1986, Gallagher et al., 1998) as well as on the beach face (Green and Black, 1999): they are called *mega-ripples*.

The genesis of these bedforms is somewhat enigmatic and their orientation and migration is not well understood (Gallagher, 2003). Ripples and megaripples may coexist, as shown in figure 2.39 where both bedforms can be clearly detected on a sea bottom exposed at low tide.

Various types of mega-ripples are observed along sandy coasts, depending on current and wave characteristics. A distinction has been proposed between mega-ripples and *hummocks*. In particular, Kleinhans et al. (2004) define hummocks as three-dimensional, low-angle bottom features which are several meters long and a few decimeters high as opposed to mega-ripples that would be steeper forms.

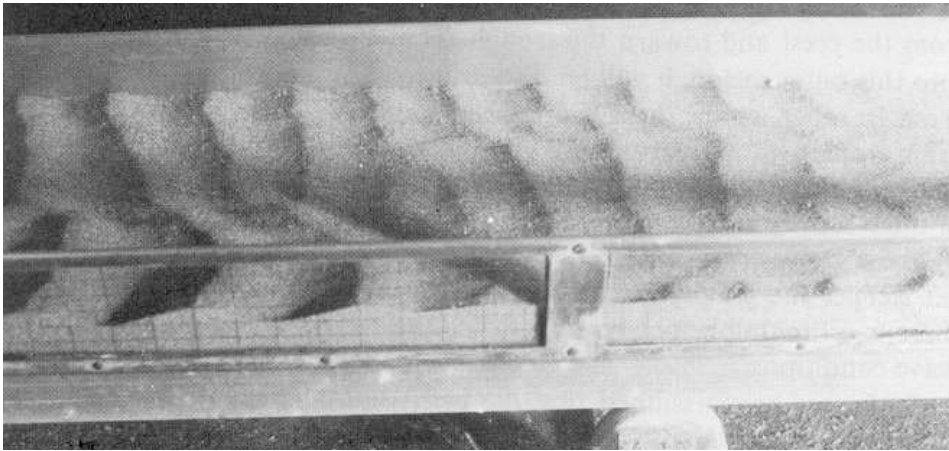


Figure 2.38: Rolling-grain ripples observed during a laboratory experiment (courtesy of John F.A. Sleath).



Figure 2.39: Megaripples at Rocky Point, Sonora, Mexico (courtesy of Ron Blakey).

Even though the origin of these bedforms is unclear, there are strong indications that they are not just large wave or current ripples but a genuinely distinct class of bedforms (Ashley et al., 1990) with a different formation mechanism.

Sand waves

In tidal environments, a mechanism similar to the ripple mechanism generates larger scale bedforms called *sand waves* or, alternatively, *tidal dunes*. Indeed, also tidal currents are oscillatory and, interacting with a wavy bottom, give rise to steady recirculating cells that drive the development of periodic bed forms characterized by much larger wavelengths. Field observations in shallow tidal seas show that the crest of sand waves are almost perpendicular to the direction of the tidal current (see figure 2.40). Moreover, their wavelengths are of the order of hundreds of meters and their amplitudes are of a few meters. These bed forms are symmetrical when the tide is dominated by one tidal constituent and the tidal current oscillates symmetrically but they become skewed when the symmetry is broken by a residual current or by the presence of further significant tide constituents.

Long bed waves

Knaapen et al. (2001) and van Dijk et al. (2008), analyzing bathymetric data of the North Sea, identified further periodic bedforms. In particular, van Dijk et al.

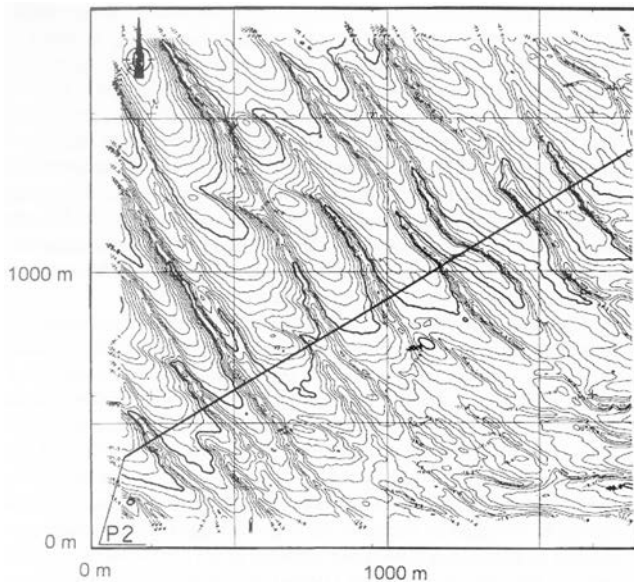


Figure 2.40: Sand waves (courtesy of SNAMPROGETTI (adapted from Besio et al. (2006)).

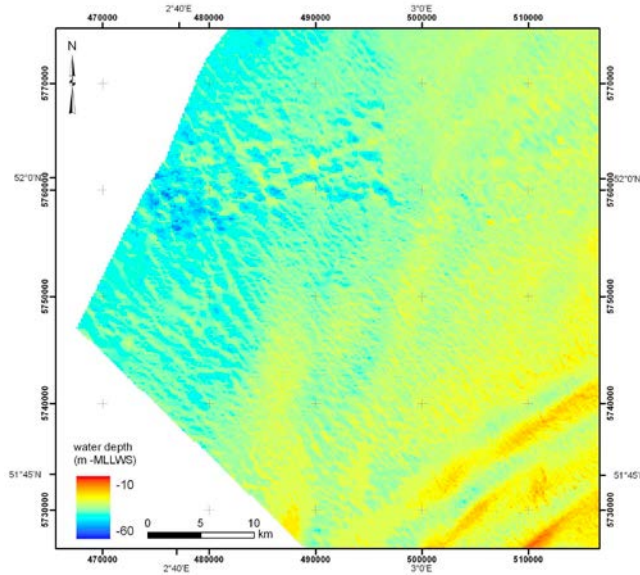


Figure 2.41: Bathymetry of the surveyed area at the offshore end of the access channel to Rotterdam harbour. The bathymetric data are provided by TNO and are compiled from measurements of the Netherlands Hydrographic Office of the Royal Netherlands Navy (courtesy of T. Van Dijk).

(2008) showed that, in the Noordhinder area, different bedforms coexist. This is shown in figure 2.41: on the left, the observed bedforms (named long bed waves after Knaapen et al. (2001)) have crests which are not orthogonal to the major axis of the tidal ellipse but are both clockwise and counter-clockwise rotated. Moreover, the crest-to-crest distance is about 1.5 km. The clockwise rotated bedforms form an angle of about 50° with the major axis of the tidal ellipse whilst the counter-clockwise rotated bedforms form an angle of about 60° . The reader should notice that, at the bottom of figure 2.41 large tidal bottom forms (*sand banks*) are also present.

Very large bed forms: sand banks and shoreface-connected ridges

Finally, in the offshore region, very large bed forms, named *tidal sand banks or tidal ridges*, are observed. Sand banks are rhythmic morphological features which are tens of meters high, tens of kilometers long and have a spacing (crest-to-crest distance) of a few kilometers. In the northern hemisphere, a typical feature of these forms is that their crests are rotated in the counter-clockwise direction with respect to the major axis of the tidal ellipse, even though this is not a strict rule as sand banks having a clockwise rotation may also be observed (Dyer and Huntley, 1999).

Similarly large periodic bedforms (*shoreface-connected ridges*) form close to the coast. Even though these features do interact with the coastline, it is appropriate to classify them as bed forms, since they have their root at the coast but extend for tens of kilometers in the offshore region. These bedforms are characterized by an alongshore spacing which can be of several kilometers. Moreover, usually, they are oblique with respect to the coastline and are thus called *shoreface-connected ridges*. Often, the seaward end of the ridges is shifted upstream with respect to its shoreward end. For this reason, they are also named *up-current rotated ridges*.

2.5.2 Coastal planforms

Beach cusps

The beach face is often characterized by periodic seaward projections of sediments that are named *beach cusps*.

They are associated with the forward and backward water motion driven by wave run-up and run-down on the beach face. The alongshore spacing of cusps observed in the field ranges from less than 1 m up to ten meters. Field observations show that the smallest values of the cusp spacing are associated with short incoming waves (small wave periods) and the cusp spacing increases with increasing lengths of the incoming waves (see figure 2.42).



Figure 2.42: A well developed reflective beach containing high tide beach cusps at Hammer Head, south Western Australia. Courtesy of Andrew D. Short.

Crescentic forms

Very long undulations of the coastline may develop during storms, when periodic horizontal recirculating cells appear in the surf region and shape the coastline and the longshore bar (see figure 2.43). Sometimes the steady offshore current gives rise to a strong jet named *rip current* (see figure 2.44), able to transport a large amount of sediment towards the open sea.

The *crescentic forms* which characterize the outer bar can be quite long (hundreds of meters) while the inner bars are segmented by shorter periodic forms (see figure 2.45). The shape of the crescentic bars is generally symmetric, but when a significant longshore current is present, the bottom patterns are skewed.



Figure 2.43: Shoreline at the western end of Pensacola Beach (FL) in March 2007. Note the presence of rhythmic crescentic forms with a characteristic wavelength of about 900 m far from the beach, along with rhythmic patterns with wavelengths of about 60 to 120 m close to the beach (courtesy of Albert E. Browder and William L. Reilly (Browder and Reilly, 2008)).

Welded bars

As already pointed out, quite often, sea waves build up a ridge of sand, gravel, or mud (*longshore bar*) which runs parallel to the shore. The longshore bar is usually submerged but it may be exposed at low tide.

The longshore periodic currents (e.g. rip-currents) may deform the longshore bar such to give it a crescentic form. The deformation is sometimes so large that the crest of the bar touches the shoreface and the longshore current generates skewed bedforms known as *welded or transverse bars* (figure 2.46).



Figure 2.44: Beach cusps and rip currents at Tunque, Chile (courtesy of Cecilia and Randy Lascody).

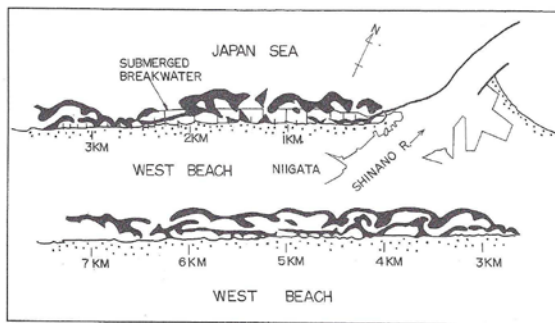


Figure 2.45: Crescentic forms observed along the Japanese coast (adapted from Hom-ma and Sonu (1962)).



Figure 2.46: Welded bars at Truc Vert beach near Arcachon, France (courtesy of Philippe Larroud'e-Tasei, LEGI, University Grenoble Alpes).

2.5.3 Grain-sorting in coastal patterns

Finally, we note that sediment heterogeneity also affects coastal patterns and gives rise to sorting phenomena similar to those observed in fluvial environments (see figure 2.47). As an example, field observations along the continental shelf adjacent to the Belgium coast, show that the sediment is usually coarser at the crests and finer at the troughs of the sand banks generated by tidal currents. Moreover, sorting affects the dynamics of bedforms. In particular, coastal ripples in well sorted sediments turn out to be shorter than those associated with a poorly sorted sediment. Similarly, the sand waves generated by a tidal current acting on a heterogeneous sediment bed are longer/shorter than those generated when the bottom sediments are well sorted, depending on the characteristics of the sediment mixture and the strength of the tidal current. Figure 2.48 shows an example



Figure 2.47: Grain sorting observed along the face of La Secca beach (Moneglia, Genoa) after a storm in August 2011 (courtesy of Eva Blondeaux).

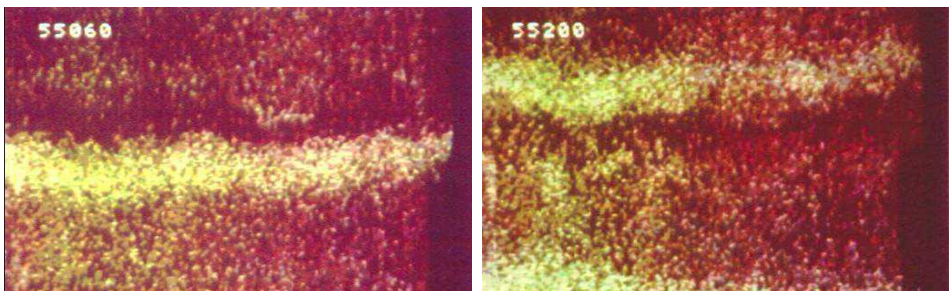


Figure 2.48: Grain sorting over ripples. The yellow sediment grains are coarser than the red sediments and pile up at the crests of the ripples which are generated in a U-tube by an oscillatory flow. The figure shows a top view of the bottom at two different phases of the cycle (adapted from Foti and Blondeaux (1995)).

of the sorting process generated by ripples. However, to the best of our knowledge, unlike in fluvial environments, no pattern generated by grain sorting (i.e. such that it would not develop if sediments were perfectly uniform) is observed in the coastal environment.

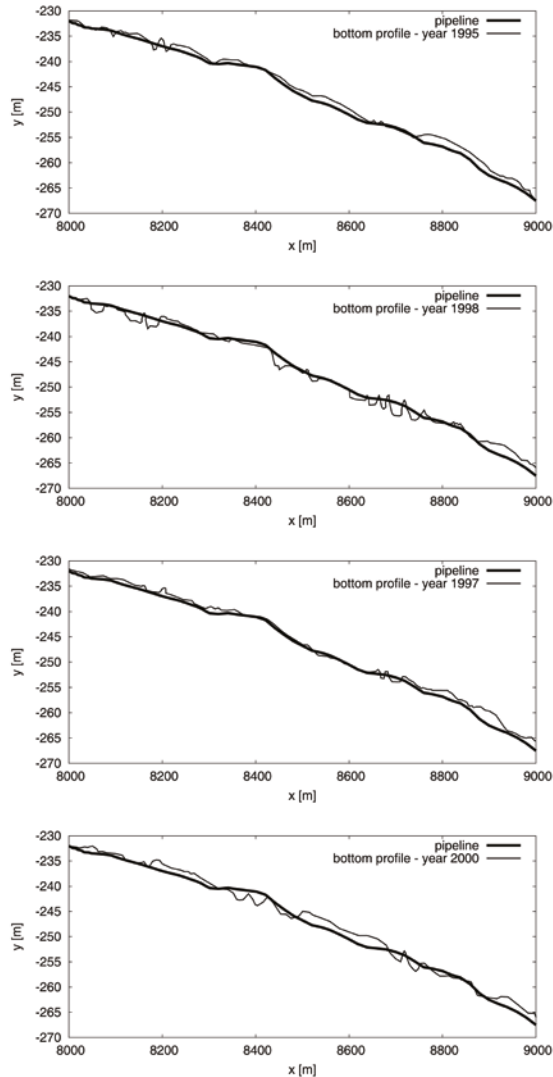


Figure 2.49: Bottom elevation measured during field surveys carried from 1995 to 2000 and profile of a pipeline (black line) which crosses the Messina Strait (courtesy of Luca Cavallaro). A significant part of the pipeline, initially buried within the seabottom, was found to be exposed due to the formation of migrating sand waves.

2.5.4 The impact of sedimentary patterns on coastal management

The formation and development of coastal patterns is of course a subject of great interest for geomorphologists. However, coastal patterns also interact in different ways and to varying degrees, with human activities. As such, they are also of major impact to coastal management.

A striking example is that of tidal sand waves. As discussed above, these forms are generated by tidal currents in shallow seas and are characterized by wavelengths of the order of hundreds of meters, heights that can reach tens of meters and migration speeds of the order of tens of meters per year. The latter feature may cause the exposure and buckling of pipelines (figure 2.49) and/or cables initially buried into the sea bed. Moreover, it may reduce the local water depth below the minimum value required for navigation (figure 2.50) and may be a source of risk for the stability of oil platforms and windmill farms (figure 2.51). The relevance of these problems can be fully appreciated noting the severe impact on the ecology of coastal environments induced by the breaking of an oil pipeline and the cost of the periodical dredging activities required to maintain navigation channels.

Similar impact is associated with sand banks. Because of their size (their wavelength is of the order of kilometers and their height is a significant fraction of the

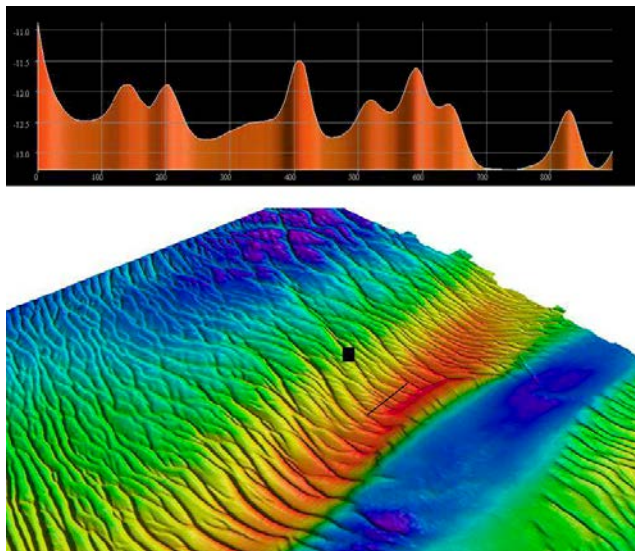


Figure 2.50: Sand wave field on the continental shelf off the Belgium coast. The figure also shows the presence of a navigation channel cut through the sand wave field. This channel has to be periodically dredged such to allow for the navigation of large ships sailing through this shallow coastal area. The top plate shows a sample of the bottom profile of a cross section cutting the sand wave field. The location of the cross section is shown in the bottom plate (black line). Its length is about 1000 m and its bottom elevation falls approximately in the range (-11.5) – (-13.25) m (courtesy of Vera Van Lanker).



Figure 2.51: Sheringham Shoal offshore wind farm, photo by Harald Pettersen/Statoil, NHD-INFO [CC-BY-2.0].

local water depth), sand banks lend themselves as ideal locations for sand mining, increasingly needed to realize large infra-structural projects. However, this practice must be subject to careful scrutiny as it may lead to undesirable effects. Indeed, large offshore sand pits, with sizes of the order of kilometers and depths of several meters, have significant direct effects on coastal morphology as well as on their ecology and biology. Moreover, there may be a further indirect impact on the far field on time scales of the order of centuries because of the interaction between waves, currents, sediment transport and seabed morphology. Ascertaining the long-term impact that extracting large quantities of sand from the crest or the trough of a sand bank would have on the coast is an unsettled issue from both a qualitative and quantitative point of view.

Some coastal patterns may also be a source of risk for swimmers. In particular, longshore crescentic forms generate the so called rip currents, directed away from the shore and cut through the breaker line. Depending on the beach geometry and wave climate these cross-shore currents can be strong, localized, and narrow thus being hazardous to inexperienced swimmers that, caught in a rip current, may be transported away from the beach. Indeed, swimming against the current is quite difficult as these currents are very strong. For this reason, in USA swimmer drowning caused by rip currents is unfortunately quite common, leading to several deaths each year.

Even small scale morphological features such as sea ripples have a number of effects of practical relevance. In fact, ripples play an important role in the mechanisms controlling sediment transport and mixing processes close to the sea bottom. Indeed, the boundary layer generated by surface waves close to the bottom separates at their crests and vortices are generated which increase mass and momentum transfer. Hence, a prerequisite for process based computational models developed to investigate large scale phenomena is the knowledge of the geometrical characteristics (wavelength and height) of ripples, required to provide reliable estimates of sediment transport and flow resistance.

2.6 Deep sea patterns

As mentioned in Section 1.2, the erosive action of turbidity currents is responsible for the numerous incisions observed along the continental shelf (figure 1.19).

In particular, small canyons are typically produced by turbidity currents close to the shelf margin and, moving downslope, they merge giving rise to larger and

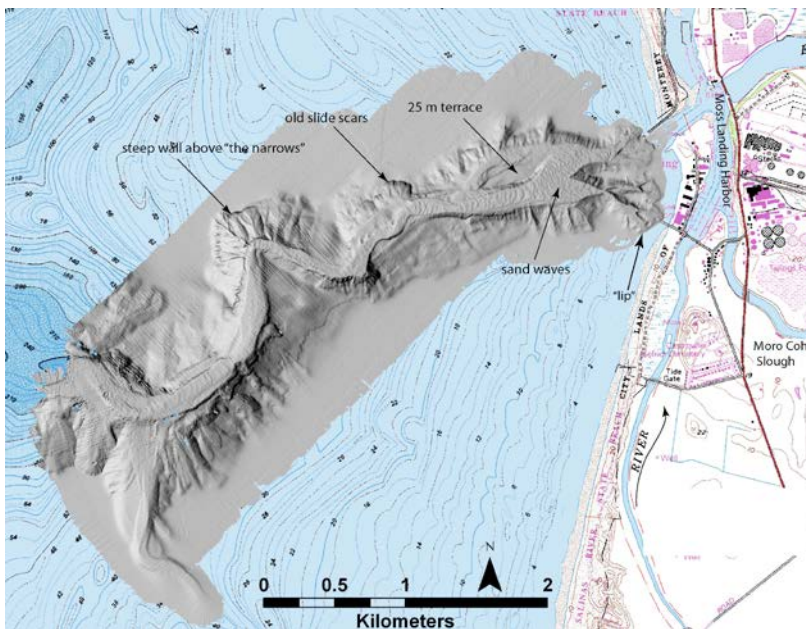


Figure 2.52: Meandering channel incised in the submarine alluvial fan generated by turbidity currents at the foot of the shelf in front of the city of Monterey (California, USA). Note also the presence of sand dunes (from *Marine Geomorphology: Geomorphic Processes, Hazards, and Paradoxes in Monterey Canyon*, authors: Douglas Smith, <https://serc.carleton.edu/vignettes/collection/37620.html>).

deeper canyons. Sediments delivered by these currents form huge submarine fans at the foot of the shelf. Fans are incised by channels that may be hundreds of kilometers long and exhibit natural levees generated by the overspilling of turbidity currents and the resulting deposition of the suspended load. These channel-levee systems are quite peculiar geomorphological features.

A number of features of fluvial and transitional patterns are also observed in the submarine environment. In particular, submarine channels are often characterized by a significant sinuosity that may be associated with low amplitude bends or highly sinuous loops. An example is reported in figure 2.52 which shows a meandering channel in front of Monterey city (California, USA).

As in alluvial rivers, the curvature of the channel axis gives rise to significant secondary currents, although their structure is not identical to their fluvial counterpart and is not fully understood yet. Erosion of the outer bank and deposition



Figure 2.53: Magnified views of figure 2.52 clearly showing the presence of sand waves (courtesy of the Seafloor Mapping Lab at California State University Monterey Bay).

at the inner bank is also observed and may lead to significant lateral channel migration.

Also the longitudinal bed profiles of turbidity currents display morphological patterns similar to those observed in fluvial environments: in particular, large scale bedforms (sand waves) somewhat similar to dunes are often observed in submarine channels (see figure 2.53 which is a larger scale view of the channel shown in figure 2.52).

Finally, the sea bed shaped by turbidity currents shows the presence of periodic bed-forms somewhat similar to those observed in mountain creeks. Figure 2.54 shows a plot of the sea bottom close to the Shepard Meander offshore the Monterey bay.

The pattern consists of a rhythmic sequence of long, weakly sloping, reaches followed by quite short reaches characterized by large slopes. This pattern is reminiscent of fluvial *cyclic steps*. Sequences of steps are displayed also in figure

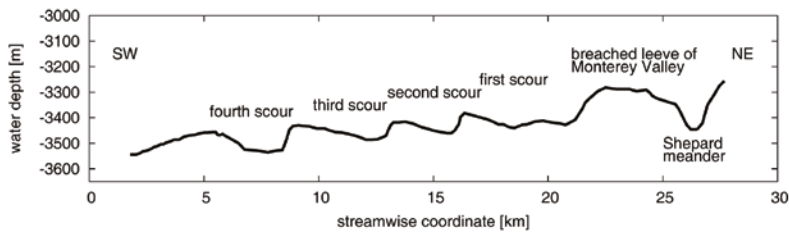


Figure 2.54: Sequence of steps observed close to the Shepard Meander, offshore of Monterey bay (adapted from Fildani et al. (2006)).

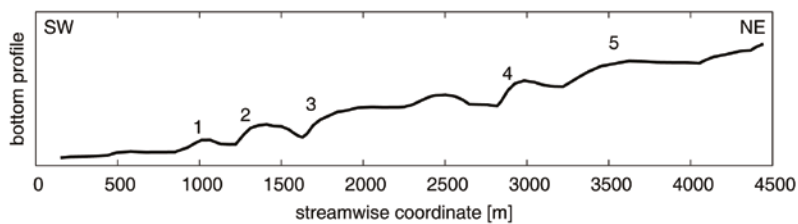


Figure 2.55: Sequence of steps observed along the San Mateo submarine channel. The bedforms are labelled 1 to 5 (adapted from Covault et al. (2014)).

2.55 that shows the bottom profile of the San Mateo submarine channel and in figure 2.56 that depicts the West Penghu and South Taiwan Shoal canyons where these periodic patterns are characterized by wavelengths ranging from 1.2 km to 10.0 km and heights from 5.4 m to 80.9 m. As described by Zhong et al. (2015),

these features are aligned with the canyon thalweg and form trains of up to 19 cyclic steps extending up to 100 km in length. The wavelength of these steps is smaller in the upper region, where the slope is higher, and larger in the lower region characterized by gentler slopes.

Different mechanisms have been proposed to explain the formation of these features but the cyclic step hypothesis is becoming the most favored. Repetitive surveys carried out along different channels suggest that these bed forms migrate upstream, a conclusion further supported by very recent field observations of Clarke (2016).

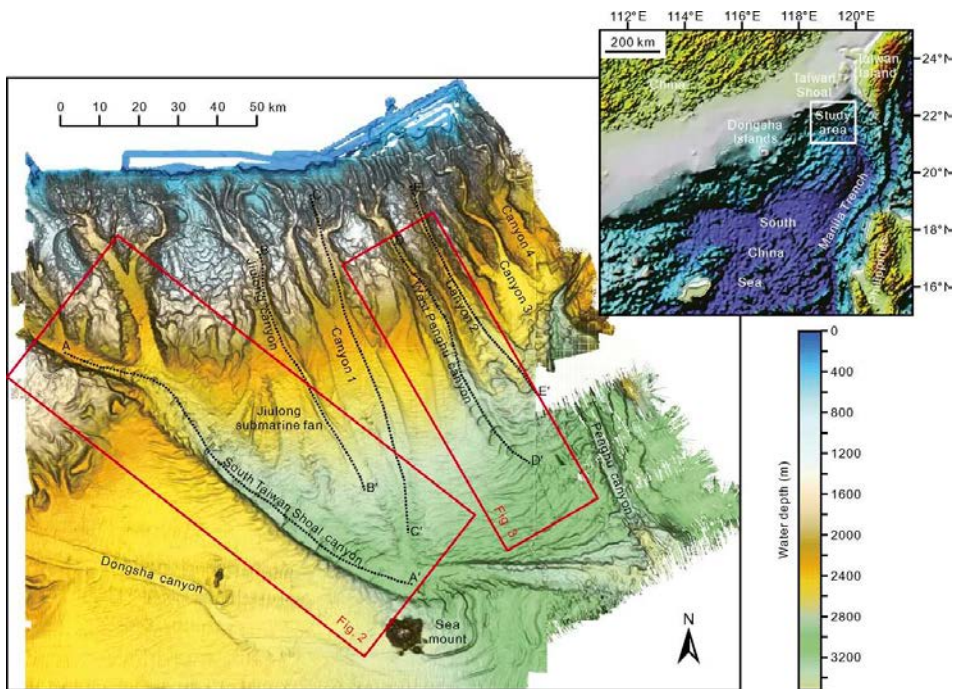


Figure 2.56: Canyons at the shelf margin of the South China Sea. A careful analysis of the topography of the West Penghu canyon allows to identify a sequence of steps. Less evident steps can be observed also along the South Taiwan Shoal canyon (<http://gsbulletin.gsapubs.org/content/127/5-6/804/F1.large.jpg>).

Even though the above picture might lead to conclude that the dynamics of turbidity currents is similar to that of their riverine counterparts, however significant differences are also recognized. In particular, the driving mechanism of turbidity currents differs from fluvial currents: it is sediment motion that drags the water and creates a stream that is virtually unconfined in the vertical direction.

Also, field observations are more difficult in the submarine case as turbidity

currents take place at very large water depths and are characterized by very large and irregular occurrence intervals. Fortunately, measurements carried out in laboratory experiments are less prohibitive and are starting to reveal details of the main mechanisms that drive the formation and evolution of turbidity currents, thus shedding some light on the origin of the morphological patterns outlined above.

2.6.1 Deep sea patterns and offshore engineering

The study of turbidity currents is of major practical relevance in the context of offshore engineering. Offshore infrastructures are increasingly needed due to the development of oil and gas pipelines laid across continental shelves: the coasts of western Africa, gulf of Mexico, Philippines as well as the coasts of large enclosed water bodies like the Caspian sea and the Black sea are regions that see a vast concentration of such infrastructures (figure 2.57). Moreover, ITC networks are interconnected through cables that are often laid down in submarine environments.



Figure 2.57: The sight of the Gulf of Mexico from the Louisiana coast at Fourchon beach. Louisiana has one of the largest concentration of oil-gas platforms (50,000) as well as oil-gas pipelines (15,000 Km) (photo by Sean Gardner, USA TODAY).

For these infrastructures turbidity currents turn out to be a severe threat. This has been known since the early work of Heezen and Ewing (1952) who documented the generation of a gigantic turbidity current generated by the Grand Banks earthquake occurred in 1929 at the continental slope south of Newfoundland in the North Atlantic. The current swept away all the telegraph cables lying downslope of the epicenter and spread over an area reaching as far as 450 miles

from the continental slope (figure 2.58). The estimated speed of the current ranged from over 25 m/s at the upper portion of the continental shelf (slope around 0.5 %) to 6 m/s at the gentling sloping oceanic floor (slope around 0.05 %).

Any intervention required for repairing possible damage in equipment laid on the deep sea is both difficult and costly. As pointed out by Bruschi et al. (2006): *"This calls for a comprehensive design basis from early stage to meet the restrictive design requirements to ensure reliability and cost effectiveness of the infrastructure over the operating life-span"*.

Sediments accumulated by turbidity currents in submarine fans over periods of the order of tens of thousands to million years may reach volumes up to millions of Km^3 (Weimer et al. (2007)). Lithification of turbidity sediments in geologic times leads to the formation of sedimentary rocks called *turbidites*. The organic material trapped in turbidity sediments is the source of hydrocarbon formation, whereby these rocks develop into huge hydrocarbon reservoirs. In order to appreciate the practical relevance of these reservoirs, it is of interest to quote the appraisal of turbidite fields made by Pettingill (1998): *"...In the 75 years from*

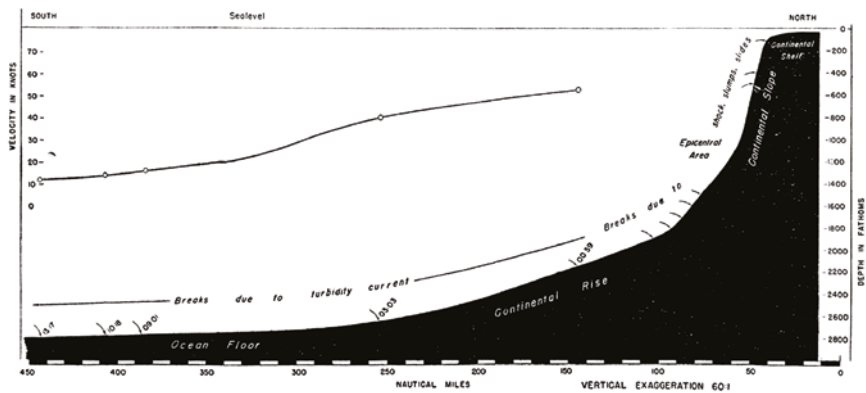


Figure 2.58: The bottom profile south the Cabot Strait and the speed of the turbidity current generated by the Grand Banks earthquake occurred in 1929 at the continental slope south of Newfoundland in the North Atlantic. The current speed is estimated from the successive cable breaks detected at different locations. Speeds are in knots (1 Knot = 1.852 Km/h) (reproduced from Heezen and Ewing (1952), figure 2).

1894-1969, approximately 14 billion BOE ultimate recoverable was discovered in 11 turbidite giants. In contrast, in the 28 years since 1970, an additional 34 billion BOE has been added in 30 giants, demonstrating a relatively recent rise in importance of turbidites as hydrocarbon reservoirs (figure 2.59)...". The Author's conclusion was: ".....turbidites are in an immature exploration stage globally and will thus play a significant role in the future of hydrocarbon exploration and production...."

Turbidity currents are also the main vectors of reservoir sedimentation, a process that has a major practical implication as it leads to progressive reduction of water storage. In order to appreciate the importance of this issue it may be of interest to quote some estimates reported by ICOLD, the International Commission for Large Dams:

- The total world reservoir storage, including small ($< 15m$) dams, is about 7000 billion m^3 , of which 3000 is dead storage for hydropower dams, 3000 are active storage devoted to hydropower and about 1000 are devoted to irrigation dams, potable or industrial water storage and multipurpose dams. Reservoir distribution among different countries is plotted in figure 2.60.

- The overall sediment stored in world reservoirs has been evaluated as 2000 billion m^3 for dams 35 years old on average: hence, a volume around 57 billion m^3 was accumulated annually in those dams. This amounts to 0.8 % of the total storage per year.

- The total yearly impact of siltation of the world's reservoirs was estimated at 21 billion \$, including annual loss of power supply and irrigation capacity, to compare with an overall yearly benefits of 175 to 225 billion \$.

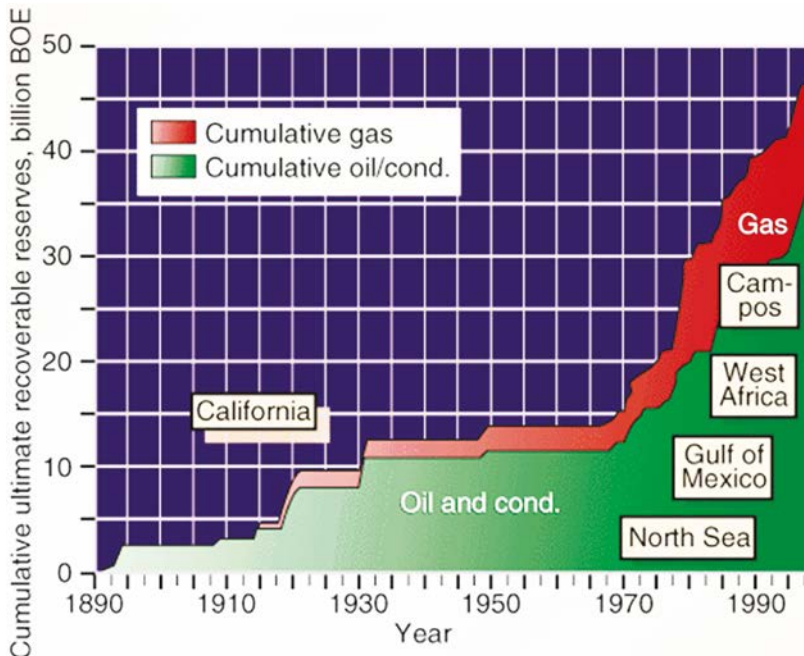


Figure 2.59: Oil and gas reserves from giant turbidity fields discovered since 1894 (reproduced from Pettingill (1998), figure 2). The barrel of oil equivalent (BOE) is a unit of energy based on the approximate energy released by burning one barrel (42 U.S. gallons or 158.99 litres) of crude oil.

- A great attention to siltation is justified by its high cost. This will also affect future dams which are planned in areas typically characterized by high sedimentation.

- Understanding the dynamics of turbidity currents is a fundamental tool to design appropriate flushing techniques to achieve mitigation of the sedimentation process.

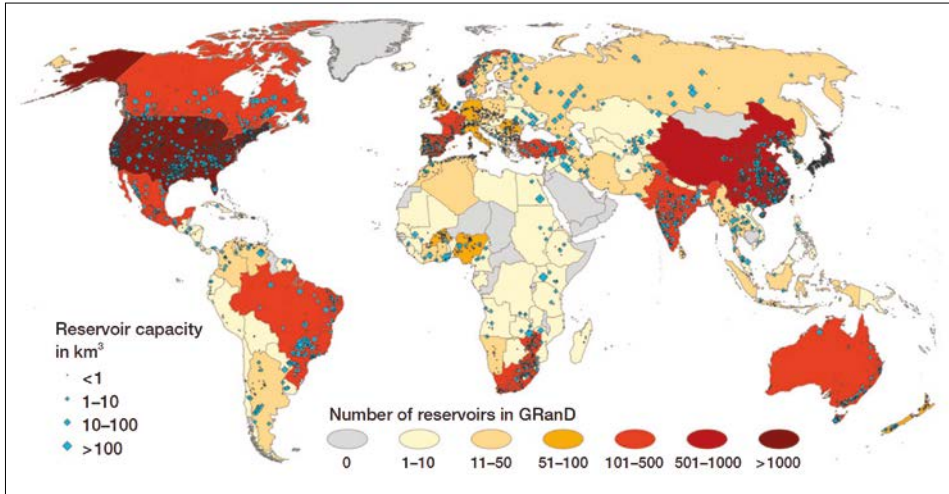


Figure 2.60: Global distribution (by country) of large reservoirs included in the Global Reservoir and Dam database (GRanD) (reproduced from Lehner et al. (2011), source: GWSP Digital Water Atlas (2008). Map 81: GRanD Database (V1.0). Available online at <http://atlas.gwsp.org>).

Chapter 3

Morphodynamics: a free boundary problem

3.1 The bed interface as a free boundary

The general problem investigated in the monographs is the formation of sub-aqueous sedimentary patterns, hence we must analyze the gravitationally driven motion of water bounded by a free surface and by a granular medium. Here, we derive the fundamental tool needed to model the dynamics of the interface fluid-granular medium which controls the formation and development of sedimentary patterns.

The analysis presented below is not restricted to a specific sedimentary environment, being equally relevant to fluvial, tidal, coastal or submarine environments. It is similarly irrelevant at this stage to define the precise nature of the erodible medium: it may be cohesionless or cohesive, coarse (gravel, sand) or fine (silt, clay).

The flow, referred to a fixed Cartesian reference frame (x_1, x_2, x_3) with x_3 vertical coordinate pointing upwards, is invariably defined in the domain $\eta < x_3 < h$, where $\eta(x_1, x_2, t)$ and $h(x_1, x_2, t)$ are the elevations of the water-medium interface and of the free surface respectively, whilst t is time. The erodible medium fills up the region $x_3 < \eta$ (figure 3.1).

The interface separating the fluid from the adjacent erodible medium, where sediment particles are at rest, is a *free boundary*: this implies that *the shape of the boundary is a priori unknown*, it depends on the characteristics of the flow field. The free nature of the interface liquid-granular medium originates from a mechanism different from that characterizing a free surface (i.e. a water-air interface). At a free surface, at each instant, the water flux as well as the air flux through the surface must vanish: this is the well known kinematic condition constraining the free surface to be a *material surface*. On the contrary, the interface between a stream and a granular medium allows for the exchange of sediment particles between the two media: solid particles belonging to the granular medium may be entrained

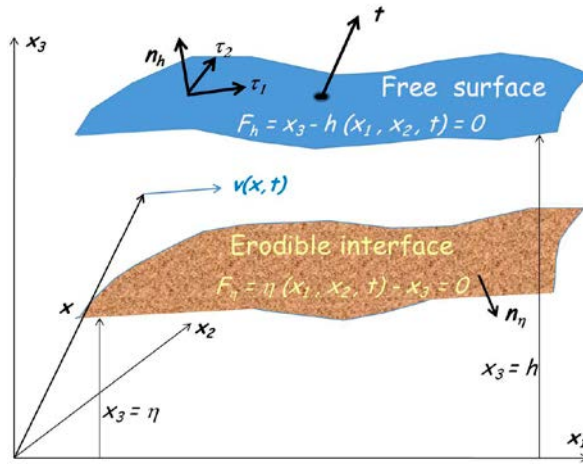


Figure 3.1: Sketch of the flow domain bounded by a free erodible interface and by the free surface.

by the stream and, conversely, solid particles transported by the stream may be deposited over the interface through various mechanisms. The two processes of entrainment and deposition coexist and balance each other exactly under conditions of equilibrium, met in a uniform stream fed by sediments at a rate exactly equal to the transport capacity of the stream.

Whenever, the latter conditions are not met, due either to non uniformity of the flow field or to insufficient/excessive sediment supply, entrained flux and deposited flux do not balance exactly and it is precisely *the difference between the two which drives a displacement of the interface and determines its free nature*. The motion of the bed interface must satisfy an evolution equation which interprets this physical mechanism.

3.2 Evolution equation of an erodible interface (Exner equation)

Particles lying on the erodible interface are subject to hydrodynamic forces which may force them to be entrained by the stream. Simultaneously, particles advected by the flow, due to their excess weight, settle back on the bed. Only smallest particles keep suspended throughout their journey: they constitute the so called *wash load*. Hence, the erodible interface between the particles resting on the bottom and the flowing mixture of water and moving particles evolves as a result of the erosion and deposition fluxes. In particular, the sedimentary environment is described as *depositional (erosional)* if the erosion flux is smaller (larger) than the deposition flux.

3.3 Exner formulation of the evolution equation

A useful formulation of the evolution equation of the erodible interface (Exner equation) can be derived starting from the local (differential) form of the continuity equation of the solid phase. Let us derive it.

3.3.1 The local form of the mass conservation equation for the solid phase

We denote by $c(\mathbf{x}, t)$ the local and instantaneous value of the volumetric concentration of the solid phase, at the point $P(\mathbf{x})$ at time t with $\mathbf{x} \equiv (x_1, x_2, x_3)$. Similarly, $\mathbf{q}_s(\mathbf{x}, t)$ is the local and instantaneous value of the volumetric sediment flux ($[\mathbf{q}_s] = \text{LT}^{-1}$).

Hence, the instantaneous form of the *mass conservation equation of the solid phase* can be written noting that, in the infinitesimal time interval dt , the volume of sediment exchanged through a differential element dS of the control surface S is equal to $(\mathbf{q}_s \cdot \mathbf{n} dS dt)$, with \mathbf{n} unit normal positive in the outer direction. The integral of the latter quantity over the whole control surface S must be balanced by the rate of variation of the volume of sediment contained in the control volume: a variation driven by the rate of change of the solid concentration $(\partial c / \partial t)$ at any point within V . A simple statement of this balance leads to the sought *equation of mass conservation for the solid phase in integral form*:

$$\int_V \frac{\partial c}{\partial t} dV + \int_S \mathbf{q}_s \cdot \mathbf{n} dS = 0 \quad (3.1)$$

Transforming the surface integral of (3.1) into a volume integral through the Ostrogradski-Gauss transformation and employing the classical argument whereby the statement of mass conservation must hold for any arbitrary portion of the volume V , leads directly to the following *differential form of the equation of mass conservation for the solid phase*

$$\frac{\partial c}{\partial t} + \nabla \cdot \mathbf{q}_s = 0 \quad (3.2)$$

The equations (3.1) and (3.2) are the starting point of morphodynamics.

The equation (3.2) must be solved with appropriate boundary conditions. Boundaries are essentially movable interfaces between the flowing mixture and an adjacent medium, namely free surfaces and bed-bank interfaces. At these boundaries the sediment concentration is discontinuous. Let c_{int} and c_{ext} the volu-

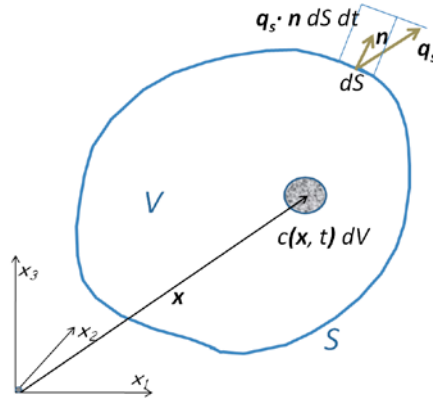


Figure 3.2: Sketch illustrating the sediment balance underlying the continuity equation of the solid phase; \mathbf{q}_s denotes the sediment flux vector.

metric concentrations at the inner and outer face of the boundary respectively: c_{ext} vanishes if the interface is a free surface and it equals the packing concentration of the erodible medium c_M at bed interfaces. Moreover, let V_n and $(\mathbf{q}_s \cdot \mathbf{n})$ denote the normal component of the velocity of the interface and the sediment flux at the interface respectively.

Then, the boundary condition at the interface S_i takes the following form:

$$\mathbf{q}_s \cdot \mathbf{n} = V_n (c_{int} - c_{ext}) \quad (\text{on } S_i) \quad (3.3)$$

having denoted by \mathbf{n} the outer unit normal at the interface. The reader may notice that the quantity $\mathbf{q}_s \cdot \mathbf{n} V_n c_{int}$ is the actual sediment flux through the moving bottom surface when the interface between the sediment at rest and the flowing mixture of water and sediment is considered.

In particular, the free surface is defined by the following equation:

$$F_h = x_3 - h(x_1, x_2, t) = 0 \quad (3.4)$$

and is characterized by unit normal \mathbf{n}_h such that:

$$\mathbf{n}_h = \frac{\nabla F_h}{|\nabla F_h|} \quad (3.5)$$

Since, c_{ext} vanishes at a free surface and c_{int} is the sediment concentration c_h at the free surface, the boundary condition (3.3) becomes:

$$\mathbf{q}_s \cdot \mathbf{n}_h = V_{nh} c_h \quad (x_3 = h) \quad (3.6)$$

with V_{nh} normal speed of the free surface.

Similarly, the bed interface is defined by the following equation:

$$F_\eta = \eta(x_1, x_2, t) - x_3 = 0 \quad (3.7)$$

and is characterized by unit normal \mathbf{n}_η (figure 3.1), such that:

$$\mathbf{n}_\eta = \frac{\nabla F_\eta}{|\nabla F_\eta|} \quad (3.8)$$

Since, c_{ext} at a bed interface equals the packing concentration of the erodible bed c_M and c_{int} is the sediment concentration c_η close to the bottom, the boundary condition (3.3) becomes:

$$\mathbf{q}_s \cdot \mathbf{n}_\eta = V_{n\eta} (c_\eta - c_M) \quad (x_3 = \eta) \quad (3.9)$$

with $V_{n\eta}$ normal speed of the bed surface.

Moving from the above formulation, we derive the Exner form of the evolution equation of the erodible interface.

3.3.2 Derivation of the 2-D Exner equation for homogeneous sediments

Exner equation is essentially a depth averaged form of the continuity equation of the solid phase. Then, we integrate equation (3.2) between the erodible interface $x_3 = \eta(x_1, x_2, t)$ and the free surface $x_3 = h(x_1, x_2, t)$ to find:

$$\int_\eta^h \frac{\partial c}{\partial t} dx_3 + \int_\eta^h \frac{\partial q_{s1}}{\partial x_1} dx_3 + \int_\eta^h \frac{\partial q_{s2}}{\partial x_2} dx_3 + q_{s3}|_h - q_{s3}|_\eta = 0 \quad (3.10)$$

Noting that the lower and the upper bounds of the integrals in (3.10) are functions of the independent variables (x_1, x_2, t) , we can use Leibnitz rule and further reduce the previous equation as follows:

$$\begin{aligned} & \frac{\partial}{\partial t} \int_\eta^h c dx_3 - c|_h \frac{\partial h}{\partial t} + c|_\eta \frac{\partial \eta}{\partial t} \\ & + \frac{\partial}{\partial x_1} \int_\eta^h q_{s1} dx_3 - q_{s1}|_h \frac{\partial h}{\partial x_1} + q_{s1}|_\eta \frac{\partial \eta}{\partial x_1} \\ & + \frac{\partial}{\partial x_2} \int_\eta^h q_{s2} dx_3 - q_{s2}|_h \frac{\partial h}{\partial x_2} + q_{s2}|_\eta \frac{\partial \eta}{\partial x_2} \end{aligned}$$

$$+q_{s3}|_h - q_{s3}|_\eta = 0 \quad (3.11)$$

Recalling the definitions (3.5) and (3.8) of the unit normals to the free surface \mathbf{n}_h and to the bed interface \mathbf{n}_η , we may employ the equations of the free surface (3.4) and of the bed interface (3.7) to obtain:

$$n_{h1} = -\frac{\partial h}{\partial x_1} n_{h3} \quad , \quad n_{h2} = -\frac{\partial h}{\partial x_2} n_{h3} \quad , \quad (3.12)$$

$$n_{h3} = \frac{1}{\sqrt{1 + \left(\frac{\partial h}{\partial x_1}\right)^2 + \left(\frac{\partial h}{\partial x_2}\right)^2}} = \frac{1}{|\nabla F_h|}$$

and similar expressions are found for the components of \mathbf{n}_η :

$$n_{\eta 1} = -\frac{\partial \eta}{\partial x_1} n_{\eta 3} \quad , \quad n_{\eta 2} = -\frac{\partial \eta}{\partial x_2} n_{\eta 3} \quad , \quad (3.13)$$

$$n_{\eta 3} = \frac{-1}{\sqrt{1 + \left(\frac{\partial \eta}{\partial x_1}\right)^2 + \left(\frac{\partial \eta}{\partial x_2}\right)^2}} = \frac{1}{|\nabla F_\eta|}$$

Furthermore, we note that the normal components of the velocity of the free surface $F_h(\mathbf{x}, t) = 0$ and erodible interface $F_\eta(\mathbf{x}, t) = 0$ read ^(°):

$$V_{nh} = -\frac{\partial F_h / \partial t}{|\nabla F_h|} = \frac{\partial h}{\partial t} n_{h3} \quad , \quad V_{n\eta} = -\frac{\partial F_\eta / \partial t}{|\nabla F_\eta|} = \frac{\partial \eta}{\partial t} n_{\eta 3} \quad (3.14)$$

Using the boundary condition (3.6) and the definition (3.14), with the help of simple algebraic manipulations, we find:

$$\left[-c|h \frac{\partial h}{\partial t} - q_{s1}|_h \frac{\partial h}{\partial x_1} - q_{s2}|_h \frac{\partial h}{\partial x_2} + q_{s3}|_h\right](n_{h3}) = -c|h V_{nh} + \mathbf{q}_s \cdot \mathbf{n}_h = 0 \quad (3.15)$$

[°]A simple derivation of the normal speed of a surface is as follows. Let $f(\mathbf{x}, t) = 0$ and $f(\mathbf{x} + d\mathbf{x}, t + dt) = 0$ be the equations of the moving surface at times t and $t+dt$. Moreover, let dn be the component of the displacement undergone by the moving surface in the direction of the unit normal \mathbf{n} in the infinitesimal time interval dt . Then we can write:

$$df = f(\mathbf{x} + dn \mathbf{n}, t + dt) - f(\mathbf{x}, t) = \frac{\partial f}{\partial n} dn + \frac{\partial f}{\partial t} dt$$

hence

$$V_n = -\frac{\partial f / \partial t}{\partial f / \partial n} = -\frac{\partial f / \partial t}{|\nabla f|}$$

Similarly, using the boundary condition (3.9) along with the definition (3.14), we obtain:

$$[c|_{\eta} \frac{\partial \eta}{\partial t} + q_{s1}|_{\eta} \frac{\partial \eta}{\partial x_1} + q_{s2}|_{\eta} \frac{\partial \eta}{\partial x_2} - q_{s3}|_{\eta}](-n_{\eta 3}) = -c|_{\eta} V_{n\eta} + \mathbf{q}_s \cdot \mathbf{n}_{\eta} = -c_M \frac{\partial \eta}{\partial t} n_{\eta 3} \quad (3.16)$$

Let us finally return to our depth integrated form of the mass conservation equation for the solid phase (3.11) using (3.15) and (3.16). With the further help of the following definitions of *depth averaged concentration* \tilde{C} and *depth integrated sediment flux* $\tilde{\mathbf{Q}}_s \equiv (\tilde{Q}_{s1}, \tilde{Q}_{s2})$ ($[\tilde{\mathbf{Q}}_s] = L^2 T^{-1}$):

$$(h - \eta) \tilde{C} = \int_{\eta}^h c dx_3 \quad , \quad \tilde{Q}_{sj} = \int_{\eta}^h q_{sj} dx_3 \quad (j = 1, 2) \quad (3.17)$$

we eventually derive the following form of the *evolution equation of the bed interface*:

$$\frac{\partial(h - \eta) \tilde{C}}{\partial t} + c_M \frac{\partial \eta}{\partial t} + \nabla \cdot \tilde{\mathbf{Q}}_s = 0 \quad (3.18)$$

where, herein, $\nabla = \left(\frac{\partial}{\partial x_1}, \frac{\partial}{\partial x_2} \right)$ is the gradient operator in two dimensions.

The equation (3.18) has a general form which is valid whatever type of sediment motion prevails in the flowing mixture. Simplified forms of (3.18) are often employed. In particular, the first term of (3.18) is often neglected, assuming that variations of the amount of sediments stored in the water column are small relative to the amount of sediments exchanged with the bed through the erodible interface. Under these conditions the evolution equation of the bed interface takes the following simpler form:

$$c_M \frac{\partial \eta}{\partial t} + \nabla \cdot \tilde{\mathbf{Q}}_s = 0 \quad (3.19)$$

The latter equation is known as the 2D Exner equation, its 1D version having first been derived by Exner (1925).

An alternative form of the equation describing the time evolution of the bed interface can be obtained by imposing a mass conservation of the solid phase and introducing the *deposition flux* \mathcal{D} as the rate at which the volume of sediments per unit horizontal area is deposited on the erodible surface and the *entrainment flux* \mathcal{E} as the rate at which the volume of sediments per unit horizontal area is entrained from the erodible medium:

$$(c_M - c_{\eta}) \frac{\partial \eta}{\partial t} + \mathcal{E} - \mathcal{D} = 0 \quad (3.20)$$

Indeed, if the elevation of the bed interface increases (decreases), there is a vertical flux of sediment $\mathcal{E} - \mathcal{D}$ through a fixed horizontal surface close to the bed and the stream above the surface should lose (gain) sediments at a rate $(c_\eta - c_M) \partial \eta / \partial t$ (figure 3.3).

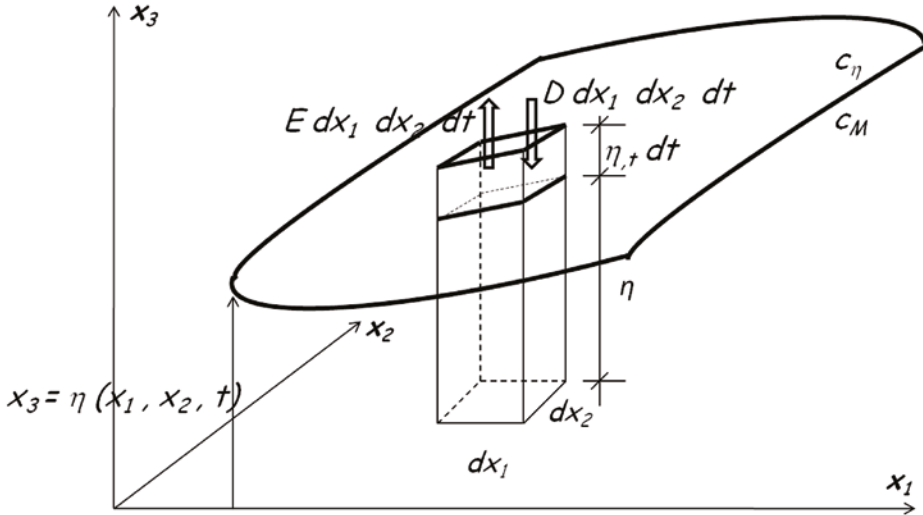


Figure 3.3: Sketch illustrating the sediment exchange fluxes between the flow and the erodible medium

A more general form of this equation, suitable to investigate sedimentary patterns evolving on very large temporal scales (say of the order of centuries), is obtained by taking into account two further phenomena that may induce variations of the bed elevation, namely *tectonic uplift* and *subsidence*. Tectonic uplift is a geological process which induces a slow increase of the elevation of the earth surface. Uplift may be the manifestation of orogeny induced by plate collisions, a process felt over a large region surrounding the colliding interface. A second mechanism is the so called isostatic uplift: the land rises as a result of weight reduction following rapid erosional removal of material from a mountain range or melting of continental glaciers and ice sheets. Subsidence is the opposite process: the elevation of the Earth surface decreases relative to the sea surface. A variety of mechanisms may cause subsidence: most notably, the dissolution of limestone by fluid flow in karst terrains, gas (or water) extraction from a natural field (an artesian aquifer) leading to reduction of the gas (water) pressure and decreasing support to the overlying soil layers, drainage induced oxygenation of peat in coastal lowlands, isostatic subsidence of the crust overloaded by deposition.

The generalized form of the evolution equation of the erodible interface reads:

$$(c_M - c_\eta) \frac{\partial \eta}{\partial t} + \mathcal{E} - \mathcal{D} = \mathcal{U} - \mathcal{S} \quad (3.21)$$

where the terms \mathcal{U} and \mathcal{S} are added to take into account the rate of the increase and decrease of the bed elevation induced by tectonic uplift and subsidence, respectively.

A sedimentary environment is more generally described as *aggradational*, *degradational* or in *morphological equilibrium* if $(\mathcal{U} + \mathcal{D})$ is larger than, smaller than or equal to $(\mathcal{E} + \mathcal{S})$.

3.3.3 Extension to the case of heterogeneous sediments

As noted in Section 1.1, sediments encountered in nature may display a significant degree of heterogeneity. In order to account for this feature in the context of morphodynamic investigations, a grain size specific statement of mass conservation for the dynamics of sediment mixtures is then required. Its formulation, however, must account for a number of processes related to the interactions between sediments of different sizes. This makes the analysis considerably more complex than in the case of the classical Exner formulation for uni-sized sediments. Let us clarify this statement.

Heterogeneity affects the mechanics of sediment transport, hence the evaluation of \tilde{Q}_s , in various ways. A first important feature is the occurrence of a process called *hiding*: smaller particles lying on the bed interface are more easily entrained due to their smaller weight but are less prone to be entrained as they tend to 'hide' in the interstices between larger particles. These two mechanisms tend to somehow balance each other. Then quantification of particle entrainment from the surface layer must be corrected for hiding. Secondly, as pointed out in Section 1.1, the surface layer of gravel bed rivers is typically significantly coarser than the substrate, i.e. the bed is *armoured*: this is observed at low flow but appears to persist at flood stage (Wilcock and DeTemple, 2005, Clayton and Pitlick, 2008). A third issue arises when transport occurs under non equilibrium conditions, leading to bed aggradation or degradation: under these conditions, an *exchange of sediments between the surface layer and the substrate* occurs. The presence of bedforms adds a major mixing mechanism to the sorting process: bedload is trapped at the troughs where transported surface material is buried as a result of bedform migration to reemerge at a later stage. This process, named *vertical sorting* (Blom et al., 2008) and the development of the variety of *sorting patterns* observed in nature have received considerable attention in the recent literature. Although the subject may hardly been described as fully settled, the importance of the topic will deserve to be the subject of a specific monograph of the present series.

3.4 Coupling the evolution of the erodible interface to the flow field

The Exner form of the evolution equation of the erodible interface involves the depth integrated components of the volumetric sediment flux. Hence, in order to make any progress, one must know the various mechanisms of sediment transport and learn how to evaluate the transport capacity of a flow. This will be the subject of a specific monograph of the series. For the present purposes, it is sufficient to appreciate that the ability of a fluid to carry sediment is essentially determined by the flow and stress fields acting on the erodible interface: in this sense morphodynamics and hydrodynamics are strictly coupled.

The time scale of the coupling process, i.e. the *morphodynamic time scale* t_M , is determined by the rate at which the bed interface is deformed as a result of the continuous exchange of sediments through it. Any particular sedimentary pattern expresses itself through a perturbation of the bed elevation, say of scale a_0 , that varies in the longitudinal direction, say over a scale l . Let us denote by Q_{s0} the scale of the intensity of the depth integrated sediment flux, a quantity that may vary widely depending on the environmental and hydrodynamic conditions. Then, Exner equation suggests that $t_M \sim \frac{a_0 l}{Q_{s0}}$. Next, let t_H be the hydrodynamic time scale, namely the temporal scale of variations of the flow field. Variations may occur as a result of external forcing, e.g. the propagation of a flood in a fluvial stream, a tidal wave in a tidal channel or sea waves in coastal regions. But even if no external forcing is present, e.g. a steady flow in a fluvial stream, the flow field must vary in order to adjust to the evolution of its boundary (the bed interface).

Then, decoupling of morphodynamics from hydrodynamics is strictly allowed provided $t_M \gg t_H$. In the past, it was customary to assume that decoupling is allowed, on the intuitive ground that bed evolution is often much slower than the response of the flow field to changes of its boundaries. However, in various recent contributions, it has been shown that, under specific conditions, decoupling may not be allowed. In particular, in the case of fluvial streams, the speed of propagation of long perturbations tends to vanish when the Froude number tends to unity. Hence, near criticality $t_H \rightarrow \infty$ and the rate of flow adjustment to the evolution of the bed interface is no longer much larger than the rate of morphodynamic evolution.

The above statements will obviously require to be more thoroughly discussed and fully justified, an effort that we will undertake in future monographs.

Bibliography

J. S. Alexander, R. C. Wilson, and W. R. Green. A brief history and summary of the effects of river engineering and dams on the Mississippi River system and delta. *US Geological Survey Circular 1375*, 43 pp, US Department of the Interior, 2012.

J. R. Allen. *Sedimentary structures, their character and physical basis. Development in Sedimentology*, 1, 592 pp, Elsevier, 1982.

A. Ashida and M. Michiue. Studies on hydraulic resistance and bed-load transport rate in alluvial streams. *Transaction Japan Society of Civil Engineering*, 206:59-69 (in Japanese), 1973.

G. M. Ashley. Classification of large-scale subaqueous bedforms: a new look at an old problem-SEPM bedforms and bedding structures. *Journal of Sedimentary Research*, 60(1): 160-172, 1990.

R. A. Bagnold. An approach to the sediment transport problem from general physics. *Geological Survey Professional Paper 422-I*, US Government Printing Office, Washington DC, 1966.

C. Baroni, A. Ribolini, G. Bruschi, and P. Mannucci. Geomorphological map and raised-relief model of the Carrara marble basins, Tuscany, Italy. *Geografia Fisica e Dinamica Quaternaria*, 33(2):233–243, 2010.

G. Besio, P. Blondeaux, and G. Vittori. On the formation of sand waves and sand banks. *Journal of Fluid Mechanics*, 557:1–27, 2006.

A. Blom, J. S. Ribberink, and G. Parker. Vertical sorting and the morphodynamics of bed form-dominated rivers: A sorting evolution model. *Journal of Geophysical Research: Earth Surface*, 113 (F01019), 2008.

P. Blondeaux and G. Vittori. Oscillatory flow and sediment motion over a rippled bed. *Proceedings of 22nd International Conference on Coastal Engineering*: 2186–2199. ASCE, 1990.

A. Browder and W. Reilly. Observations of large-scale beach cusps in the Florida panhandle and Alabama. In *Annual National Conference on Beach Preservation Technology*: 1–16, 2008.

R. Bruschi, S. Bughi, M. Spinazzè, E. Torselletti, and L. Vitali. Impact of debris flows and turbidly currents on seafloor structures. *Norwegian Journal of Geology*, 86:317–336, 2006.

J. E. H. Clarke. First wide-angle view of channelized turbidity currents links migrating cyclic steps to flow characteristics. *Nature Communications*, 7, 2016.

J. A. Clayton and J. Pitlick. Persistence of the surface texture of a gravel-bed river during a large flood. *Earth Surface Processes and Landforms*, 33(5):661–673, 2008.

M. Colombini. Turbulence-driven secondary flows and formation of sand ridges. *Journal of Fluid Mechanics*, 254:701–719, 1993.

M. Colombini and G. Parker. Longitudinal streaks. *Journal of Fluid Mechanics*, 304:161–183, 1995.

A. Corey. Influence of shape on the fall velocity of sand grains. Master of Science Thesis, Colorado A&M College. Fort Collins, Colorado, 1949.

F. Cortopassi, M. Daddi, G. D. Avanzi, R. Giannecchini, G. Lattanzi, Merlini, and P. Milano. Discariche di cava e instabilità dei versanti: Valutazione preliminare di alcuni fattori significativi nel bacino marmifero di Carrara (in Italian). *Journal of Engineering Geology and Environment. Special Issue*, 2008.

J. A. Covault, S. Kostic, C. K. Paull, H. F. Ryan, and A. Fildani. Submarine channel initiation, filling and maintenance from sea-floor geomorphology and morphodynamic modelling of cyclic steps. *Sedimentology*, 61(4):1031–1054, 2014.

R. W. Dalrymple and R. N. Rhodes. Estuarine dunes and bars. *Geomorphology and Sedimentology of Estuaries*, 53:359–422, 1995.

P. Diplas, R. Kuhnle, J. Gray, D. Glysson, and T. Edwards. Sediment transport measurements. In *Sedimentation Engineering: Theories, Measurements, Modeling, and Practice*. ASCE Manuals and Reports on Engineering Practice, 110:165–252, 2008.

K. R. Dyer and D. A. Huntley. The origin, classification and modelling of sand banks and ridges. *Continental Shelf Research*, 19(10):1285–1330, 1999.

A. Einstein. The cause of the formation of meanders in the courses of rivers and of the so-called Baer's law. *Die Naturwissenschaften*, 14(11):223–224, 1926.

F. Engelund and J. Fredsøe. Sediment ripples and dunes. *Annual Review of Fluid Mechanics*, 14(1):13–37, 1982.

F. M. Exner. Über die wechselwirkung zwischen wasser und geschiebe in flüssen. *Akademie der Wissenschaften in Wien, Mathematisch Naturwissenschaftliche Klasse, Sitzungsberichte, Abt IIA*, 134:165–203, 1925.

FAO. The state of world fisheries and aquaculture (SOFIA 2016). Fisheries and Aquaculture Department, 2016.

A. Fildani, W. R. Normark, S. Kostic, and G. Parker. Channel formation by flow stripping: Large-scale scour features along the Monterey East channel and their relation to sediment waves. *Sedimentology*, 53(6):1265–1287, 2006.

E. Foti and P. Blondeaux. Sea ripple formation: the heterogeneous sediment case. *Coastal Engineering*, 25(3-4):237–253, 1995.

S. Francalanci, E. Paris, and L. Solari. A combined field sampling-modeling approach for computing sediment transport during flash floods in a gravel-bed stream. *Water Resources Research*, 49(10):6642–6655, 2013.

V. Galay. Causes of river bed degradation. *Water Resources Research*, 19(5): 1057–1090, 1983.

E. L. Gallagher. A note on megaripples in the surf zone: evidence for their relation to steady flow dunes. *Marine Geology*, 193(3):171–176, 2003.

E. L. Gallagher, S. Elgar, and E. B. Thornton. Megaripple migration in a natural surf zone. *Nature*, 394(6689):165–168, 1998.

W. E. Galloway. Process framework for describing the morphologic and stratigraphic evolution of deltaic depositional systems. In *Deltas: models for exploration*. Broussard M.L. (Ed), Houston Geological Society: 87-98, 1975.

M. H. Garcia (Ed). *Sedimentation engineering: processes, measurements, modeling and practice*. ASCE, Manual and Reports on Engineering Practice, 110, 2008.

W. H. Graf. *Hydraulics of sediment transport*. Water Resources Publication, 1984.

M. O. Green and K. P. Black. Suspended-sediment reference concentration under waves: field observations and critical analysis of two predictive models. *Coastal Engineering*, 38(3):115–141, 1999.

B. Greenwood and D. J. Sherman. Hummocky cross-stratification in the surf zone: flow parameters and bedding genesis. *Sedimentology*, 33(1): 33–45, 1986.

A. Günter. Die kritische mittlere Sohlenschubspannung bei Geschiebemischungen unter Berücksichtigung der Deckschichtbildung und der turbulenzbedingten Sohlenschubspannungsschwankungen. PhD thesis, ETH Zürich, 1971.

C. Heezen and M. Ewing. Turbidity currents and submarine slumps, and the 1929 grand banks earthquake. *American Journal of Science*, 250(12): 849–873, 1952.

S. Higgins, I. Overeem, A. Tanaka, and J. P. Syvitski. Land subsidence at aquaculture facilities in the Yellow river delta, China. *Geophysical Research Letters*, 40(15):3898–3902, 2013.

M. Hom-ma and C. Sonu. Rhythmic pattern of longshore bars related to sediment characteristics. *Proceedings of 8th Coastal Engineering Conference*: 248-278, 1962.

P. P. Jansen, L. Van Bendegom, J. Van den Berg, M. De Vries, and A. Zanen. *Principles of River Engineering: The non-tidal alluvial river*. Delftse Uitgevers Maatschappij, 1994.

J. F. Kennedy. The formation of sediment ripples, dunes, and antidunes. *Annual Review of Fluid Mechanics*, 1(1):147–168, 1969.

M. G. Kleinhans, S. Passchier, and T. A. Van Dijk. The origin of megaripples, long wave ripples and hummocky cross-stratification in the North Sea in mixed flows. In *2nd International Conference Marine Sandwave and River Dunes Dynamics*, S. J. M. H. Hulscher and T. Garlan (Ed): 142–151, 2004.

M. A. Knaapen, S. J. M. H. Hulscher, H. J. Vriend, and A. Stolk. A new type of sea bed waves. *Geophysical Research Letters*, 28(7):1323–1326, 2001.

ICOLD. Sedimentation and sustainable use of reservoirs and river systems. *Bulletin Preprint 147*, International Commission on Large Dams, 2009.

B. Lehner, C. R. Liermann, C. Revenga, C. Vörösmarty, B. Fekete, P. Crouzet, P. Döll, M. Endejan, K. Frenken, J. Magome, et al. High-resolution mapping of the world's reservoirs and dams for sustainable river-flow management. *Frontiers in Ecology and the Environment*, 9(9): 494–502, 2011.

L.B. Leopold and M. G. Wolman. River channel patterns: braided, meandering, and straight. *US Geological Survey Professional Paper 282-B*, US Government Printing Office, Washington DC, 1957.

Louisiana Department of Natural Resources. Coastal restoration Annual Project Reviews, December 2003.

M. Lvovich, G. Y. Karasik, N. Bratseva, G. Medvedeva, and A. Maleshko. Contemporary intensity of the world land intracontinental erosion. USSR Academy of Sciences, Moscow, 1991.

R. H. Meade and J. A. Moody. Causes for the decline of suspended-sediment discharge in the Mississippi river system, 1940–2007. *Hydrological Processes*, 24(1):35–49, 2010.

L. R. Oldeman, R. T. A. Hakkeling, and W. G. Sombroek. World map of the status of human-induced soil degradation: an explanatory note, 2nd. rev. *Technical Report*, International Soil Reference and Information Centre, Nairobi, 1991.

R. K. Pachauri, M. R. Allen, V. R. Barros, J. Broome, W. Cramer, R. Christ, J. A. Church, L. Clarke, Q. Dahe, P. Dasgupta, et al. Climate change

2014: Synthesis Report. Contribution of Working Groups I, II and III to the *Fifth Assessment Report* of the Intergovernmental Panel on Climate Change, 2014.

G. Parker and A. W. Peterson. Bar resistance of gravel-bed streams. *Journal of the Hydraulics Division*, ASCE, 106(10):1559–1575, 1980.

D. Parsons, J. Best, O. Orfeo, R. Hardy, R. Kostaschuk, and S. Lane. Morphology and flow fields of three-dimensional dunes, Rio Paraná, Argentina: Results from simultaneous multibeam echo sounding and acoustic doppler current profiling. *Journal of Geophysical Research: Earth Surface*, 110 (F4), 2005.

H. S. Pettingill. Lessons learned from 43 turbidite giant fields. *Oil and Gas Journal*, 96(41):93–95, 1998.

M. Rinaldi. Studio geomorfologico dei principali alvei fluviali nel bacino del fiume Magra finalizzato alla definizione delle linee guida di gestione dei sedimenti e della fascia di mobilità funzionale. *Technical Report (in Italian)*, University of Florence, Department of Civil Engineering, 2005.

G. Seminara. Effect of grain sorting on the formation of bedforms. *Applied Mechanics Reviews*, 48(9):549–563, 1995.

G. Seminara, M. Colombini, A. Siviglia, and B. Federici. Modellazione idraulica, studi e valutazioni sul trasporto solido lungo l’asta del fiume Tanaro. *Technical Report (in Italian)*, University of Genoa, DICCA, 2003.

G. Seminara, M. B. Pittaluga, and R. Luchi. Attività di studio della morfodinamica del fiume Magra e degli affluenti principali in relazione all’evento alluvionale del 25 ottobre 2011 e definizione delle azioni e degli interventi di messa in sicurezza. *Technical Report (in Italian)*, University of Genoa, DICCA, 2012.

J. D. Smith. Stability of a sand bed subjected to a shear flow of low Froude number. *Journal of Geophysical Research*, 75(30):5928–5940, 1970.

J. Sui, Y. He, and B. Karney. Flow and high sediment yield from the Huangfuchuan watershed. *International Journal of Environmental Science & Technology*, 5(2):149–160, 2008.

D. J. R. Swift, A. G. Figueiredo Jr, G. L. Freeland, and G. F. Oertel. Hummocky cross-stratification and megaripples: a geological double standard. *Journal of Sedimentary Research*, 53(4): 1255-1317, 1983.

J. P. M. Syvitski and Y. Saito. Morphodynamics of deltas under the influence of humans. *Global and Planetary Change*, 57(3):261–282, 2007.

H. Vân and S. Moffett. The quiet sinking of world's deltas. <http://www.futureearth.org/blog/2014-apr-4/quiet-sinking-worlds-deltas>, 2014.

J. Van de Meene, J. Boersma, and J. Terwindt. Sedimentary structures of combined flow deposits from the shoreface-connected ridges along the central dutch coast. *Marine Geology*, 131(3-4):151–175, 1996.

T. A. van Dijk, R. C. Lindenbergh, and P. J. Egberts. Separating bathymetric data representing multiscale rhythmic bed forms: A geostatistical and spectral method compared. *Journal of Geophysical Research: Earth Surface*, 113(F4), 2008.

V. A. Vanoni. *Sedimentation engineering*, ASCE Manuals and Reports on Engineering Practice 54, 1975.

D. E. Walling and B. Webb. Patterns of sediment yield. In *Background to Palaeohydrology*: 69–100, Wiley, 1983.

D. E. Walling and B. Webb (Ed). Erosion and Sediment Yield: Global and Regional Perspectives. Proceedings of an *International Symposium*, Exeter UK, 15th-19th July 1996, IAHS publication 236, 1996.

T. Waltham. The flooding of New Orleans. *Geology Today*, 21(6):225–231, 2005.

P. Weimer, R. M. Slatt with R. Bouroullec, R. Fillon, H. Pettingill, M. Pranter, and G. Tari. *Introduction to the petroleum geology of deepwater settings*, AAPG Studies in Geology 57, American Association of Petroleum Geologists, 2006.

C. K. Wentworth. A scale of grade and class terms for clastic sediments. *The Journal of Geology*, 30(5):377–392, 1922.

P. J. Whiting, W. E. Dietrich, L. B. Leopold, T. G. Drake, and R. L. Shreve. Bedload sheets in heterogeneous sediment. *Geology*, 16(2):105–108, 1988.

P. R. Wilcock and B. T. DeTemple. Persistence of armor layers in gravel-bed streams. *Geophysical Research Letters*, 32(8), L08402, 2005.

G. P. Williams and M. G. Wolman. Downstream effects of dams on alluvial rivers. *Geological Survey Professional Paper* 1286, US Government Printing Office, Washington DC, 1984.

B. R. Winkley. Man-made cutoffs on the lower Mississippi River, conception, construction, and river response. *Technical report*, DTIC Document, 1977.

J. Xu, O. E. Sequeiros, and M. A. Noble. Sediment concentrations, flow conditions, and downstream evolution of two turbidity currents, Monterey Canyon, USA. *Deep Sea Research Part I*, 89:11–34, 2014.

H. Yisan and X. Fuling. Effects of river training works on flood control. In *Taming the Yellow River: Silt and Floods*: 617–636, L. M. Brush and M. G. Wolman (Ed), Springer, 1989.

G. Zhong, M. J. Cartigny, Z. Kuang, and L. Wang. Cyclic steps along the South Taiwan Shoal and West Penghu submarine canyons on the Northeastern continental slope of the South China Sea. *Geological Society of America Bulletin*, 127(5-6):804–824, 2015.

G. Zolezzi, M. Guala, D. Termini, and G. Seminara. Experimental observations of upstream overdeepening. *Journal of Fluid Mechanics*, 531: 191–219, 2005.

Series of monographs on Morphodynamics of Sedimentary Patterns

Published monographs:

P.Blondeaux, M.Colombini, G. Seminara, and G. Vittori.
Introduction to Morphodynamics of Sedimentary Patterns.
Monograph series 'Morphodynamics of Sedimentary Patterns',
ISBN: 978-88-97752-99-8

Paolo Blondeaux graduated in Civil Engineering at the University of Genoa, where he started his academic career. Then, he became full professor, moved to the University of l'Aquila and returned to the University of Genoa in 1997. Blondeaux's research interests range over fluid mechanics, coastal hydrodynamics and morphodynamics.

Marco Colombini, graduated in Chemical Engineering at the University of Genoa in 1984, where he became full professor in 2000. He presently teaches Hydraulics and Fluvial Hydraulics in the Civil and Environmental Engineering program. Colombini's research interests span from fluid mechanics to fluvial hydraulics and morphodynamics.

Giovanni Seminara, Laurea in Civil Engineering (Genoa) and PhD in Applied Maths (Imperial College, London), formerly professor of Fluid Mechanics in Genoa University, is presently professor emeritus. Seminara's research interests focus on fluid mechanics and applications to bio-engineering, hydraulic engineering and geophysics.

Giovanna Vittori graduated in Mathematics at the University of Genoa and was awarded a PhD in Hydrodynamics at the University of Padua. Presently, she is full professor of Fluid Mechanics at the University of Genoa. Her main research interests include hydrodynamic stability, turbulence, coastal hydrodynamics and morphodynamics.

Morphodynamics is a new discipline that investigates the formation and development of *sedimentary patterns*, i.e. the shapes of the cohesionless or cohesive boundaries of water bodies, evolving in response to the action of flowing water. Sedimentary patterns occur in fluvial, transitional, coastal and submarine environments. Their fascinating forms (e.g. dunes, meanders, alluvial fans, deltas, lagoons, coastal bars, tidal ridges, submarine fans) have attracted the attention of scientists. They also play a major role in fluvial, coastal and offshore engineering.

The present monograph is the first of a series planned by an Editorial Committee comprising the four Authors. It provides a phenomenological introduction to the variety of patterns that will be investigated in the future Monographs. It also introduces to the mathematical theory of Morphodynamics, clarifying its nature of free boundary problem for the interface between a flowing water-sediment mixture and an erodible boundary.

ISBN: 978-88-97752-99-8



Copia fuori commercio